with IL-4 or IL-13 in UAMS-32 cells. Both cytokines increased OPG mRNA expression levels in similar dose- and time-dependent manners (Fig. 2a, b). Similarly, OPG protein levels in the culture supernatants of UAMS-32 cells were also increased following treatment with IL-4 and IL-13 in dose- and time-dependent manners (Fig. 2c, d). IL-4 and IL-13 have been shown to recover OPG mRNA expression down-regulated by 1α,25-$(OH)_2D_3$ in mouse calvariae and osteoblasts,[14] therefore we also examined their effects on OPG mRNA expression levels in the presence of 1α,25-$(OH)_2D_3$. Addition of the cytokines led to recovery of the down-regulation of OPG gene expression by 1α,25-$(OH)_2D_3$ (Fig. 2e). Further, the expression levels of RANKL mRNA were decreased in a similar dose-dependent manner (Fig. 2f). These results suggest that IL-4 and IL-13 act in a similar manner toward osteoblasts to stimulate the production of OPG, which inhibits osteoclast differentiation.

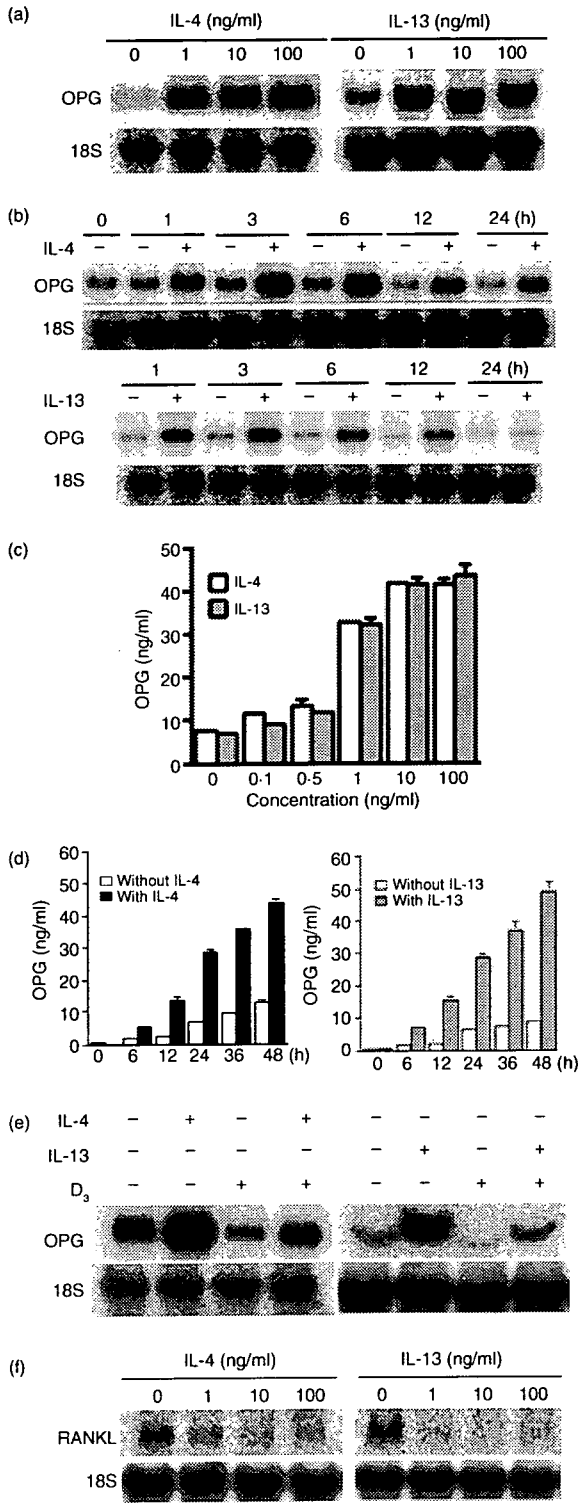

Inhibition of RANKL-induced osteoclast differentiation by IL-4 and IL-13

We next examined the direct effects of IL-4 and IL-13 on osteoclast differentiation from BMMs (osteoclast precursors) using a BMM culture system. As shown in Fig. 3(a), IL-4 at 3 ng/ml completely inhibited osteoclast differentiation induced by RANKL, while the same concentration of IL-13 demonstrated only slight inhibition and did not completely inhibit osteoclast differentiation even at a concentration of 10 ng/ml. The IC_{50} values of IL-4 and IL-13 for osteoclast differentiation were 0·34 and 13·54 ng/ml, respectively (Figs 3a,b). These results suggest that the stronger inhibitory action of IL-4 observed in our coculture system was caused by the different sensitivities of osteoclast precursors to IL-4 and IL-13.

Figure 2. Regulation of OPG and RANKL gene expression by IL-4 and IL-13 in osteoblastic cells. (a) Dose effects of IL-4 and IL-13 on the induction of OPG mRNA. UAMS-32 cells were treated with 1, 10, and 100 ng/ml of IL-4 or IL-13 for 3 hr. (b) Time course analysis of OPG mRNA expression in the presence of IL-4 or IL-13. UAMS-32 cells were treated with 10 ng/ml of IL-4 or IL-13 for 1, 3, 6, 12, and 24 hr. (c) Dose effects of IL-4 and IL-13 on the secretion of OPG protein. UAMS-32 cells were treated with 0·1, 0·5, 1, 10, and 100 ng/ml of IL-4 (white bars) or IL-13 (grey bars) for 12 hr. Data are shown as the means ± SD ($n = 3$). (d) Time course analysis of the secretion of OPG protein in the presence of IL-4 or IL-13. UAMS-32 cells were treated with 10 ng/ml of IL-4 (black bar) or IL-13 (grey bar) for 6, 12, 24, 36, and 48 hr. Concentrations of OPG in the conditioned media of UAMS-32 cells were determined by enzyme-linked immunosorbent assay. Data are shown as the means ± SD ($n = 3$). (e) Effects of IL-4 and IL-13 on OPG mRNA in osteoblastic cells pretreated with 1α,25-$(OH)_2D_3$. UAMS-32 cells were pretreated with 100 nM of 1α,25-$(OH)_2D_3$ for 1 hr, followed by treatment with 10 ng/ml of IL-4 or IL-13 for 3 hr. (f) Effects of IL-4 and IL-13 on RANKL mRNA in osteoblastic cells. UAMS-32 cells were treated with 1, 10, and 100 ng/ml of IL-4 or IL-13 for 24 hr. (a, c, e, and f) The expressions of RANKL mRNA, OPG mRNA, and 18S rRNA were detected by Northern blot analysis.

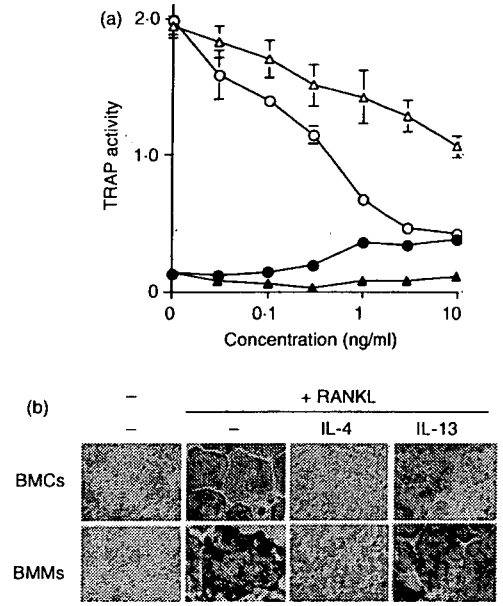

Figure 3. Effects of IL-4 and IL-13 on osteoclast differentiation induced by RANKL in osteoclast precursor cultures. (a) BMMs were cultured with various concentrations of IL-4 with (○) or without (●) 150 ng/ml of RANKL, or IL-13 with (△) or without (▲) 150 ng/ml of RANKL. After culturing the cells, the cell lysates were harvested and TRAP activity was measured. Data are shown as the means ± SE ($n = 4$). (b) Photographs of BMCs and BMMs treated with 10 ng/ml of IL-4 or IL-13. The cells were fixed and stained for TRAP (original magnification ×10).

Expression of receptor components for IL-4 and IL-13 in osteoclast precursors and osteoblasts

To explore the mechanism of IL-4 and IL-13 action, we analysed the expressions of receptor components for IL-4 and IL-13 (Fig. 4). Although IL-4Rα and IL-13Rα1 mRNAs were commonly expressed in all the cells tested, the γc mRNA was expressed in osteoclast precursors such as BMCs and BMMs but not in osteoblastic cells such as primary osteoblasts and UAMS-32 cells (Fig. 4). Consistently, the RAW264.7 cell line known as osteoclast precursors and the ST-2 stromal cell line showed the same expression patterns with BMCs/BMMs and osteoblasts/UAMS-32 cells, respectively (Fig. 4).

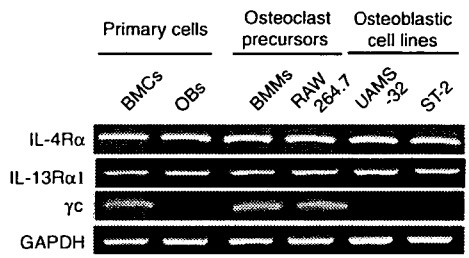

Figure 4. Expression of receptor components for IL-4 and IL-13 in osteoclast precursors and osteoblastic cells. Total RNAs were extracted from BMCs, primary osteoblasts (OBs), BMMs, RAW264.7 cells, UAMS-32 cells, and ST-2 cells. Subsequently, the mRNA expressions of IL-4Rα, IL-13Rα1, γc, and GAPDH in the cells were analysed by RT–PCR.

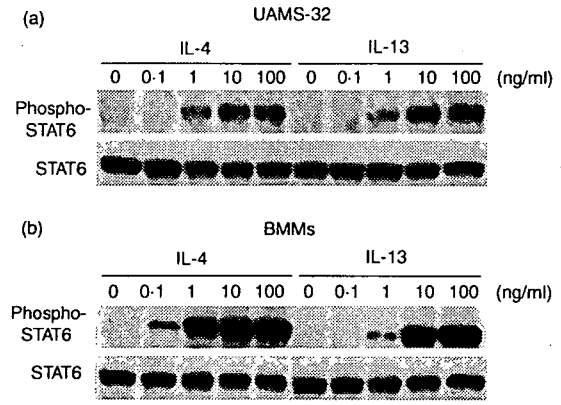

Figure 5. Phosphorylation of STAT6 by IL-4 and IL-13 in UAMS-32 cells and BMMs. UAMS-32 (a) cells and BMMs (b) were treated with 0·1, 1, 10 and 10 ng/ml of IL-4 and IL-13 for 30 min. Subsequently, phosphorylation of STAT6 protein was analysed by Western blot analysis.

Activation of STAT6 by IL-4 and IL-13 in osteoclast precursors and osteoblasts

In the UAMS-32 cells, phosphorylation of STAT6 occurred in the presence of as little as 1 ng/ml IL-4 or IL-13 and increased in a dose-dependent manner, with phosphorylation levelling off at 10 ng/ml (Fig. 5a). On the other hand, in the BMMs, phosphorylation of STAT6 occurred at lower concentrations of IL-4 (≥0·1 ng/ml) than those of IL-13 (≥ 1 ng/ml) (Fig. 5b). These results suggest that the effects of IL-4 and IL-13 on the activation of STAT6 in osteoblasts are equivalent, but IL-4 proved to be more effective than IL-13 for activation of STAT6 in osteoclast precursors.

Effects of IL-4 and IL-13 on expression of NFATc1 mRNA in osteoclast precursors

Because NFATc1 is known to be a critical gene for regulating the differentiation of osteoclasts,[19] we examined the effects of IL-4 and IL-13 on the expression of NFATc1 mRNA in BMMs treated with RANKL (Fig. 6). The expression of NFATc1 mRNA induced by RANKL in BMMs was completely inhibited by 10 ng/ml of IL-4, while the same concentration of IL-13 demonstrated only slight inhibition. This is consistent with the results observed in the BMM culture system following treatment with IL-4 and IL-13.

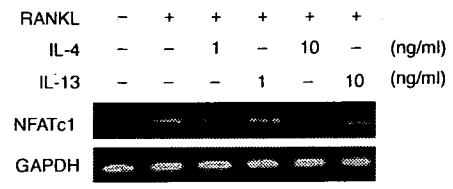

Figure 6. Effects of IL-4 and IL-13 on NFATc1 mRNA expression in osteoclast precursors. BMMs were treated with or without 150 ng/ml of RANKL in the presence of IL-4 or IL-13 at the indicated concentrations for 24 hr. Total RNA was then extracted and NFATc1 mRNA expression was examined using RT–PCR.

Discussion

It has been reported that IL-4 and IL-13 inhibit osteoclast differentiation in a similar manner.[14,20–24] However, the present results demonstrated some differences in regard to their activities toward osteoclast precursors and osteoblasts. Our data suggest that the inhibitory effect of IL-4 is stronger than that of IL-13 toward osteoclast precursors, while their effects on OPG and RANKL mRNA expression in osteoblasts are equivalent.

After comparing the IC_{50} values of IL-4 and IL-13 between the coculture and BMM culture systems, it was apparent that both cytokines inhibited osteoclast differentiation more strongly in the coculture system than in the BMM culture system, as their IC_{50} values were 0·13 ng/ml and 2·69 ng/ml, respectively, in the coculture system, and 0·34 ng/ml and 13·54 ng/ml, respectively, in the BMM culture system. These results suggest that inhibition of osteoclast differentiation by IL-4 and IL-13 is derived from not only their direct actions on osteoclast precursors, but also indirect actions on osteoblasts, including up-regulation of OPG production and down-regulation of RANKL expression.

Palmqvist *et al.* showed that IL-4 and IL-13 at a concentration of 50 ng/ml slightly increased OPG mRNA expression levels in calvarial osteoblasts after 48 hr, when evaluated using RT–PCR.[14] Our time course and dose–response results using Northern blot analysis indicated that the cytokines strongly induced OPG mRNA expression after 1 hr, even at 1 ng/ml. Further, the maximum expression levels of OPG mRNA were observed at 3 hr and decreased thereafter. These results suggest that OPG production is regulated very quickly and strongly by stimulation with IL-4 and IL-13. As for RANKL, a concentration of 1 ng/ml of IL-4 or IL-13 was enough to down-regulate its expression for 24 hr. Thus, IL-4 and IL-13 may regulate OPG and RANKL production in osteoblasts to inhibit osteoclast differentiation in a manner more sensitive than previously supposed.

In the immune system, IL-4 is necessary for $CD4^+$ Th2 cell development, while IL-13 has been reported to have negligible effects on T cells.[25] These functional differences have been explained by the different expression patterns of the receptor subunits.[26] The present results showed that IL-4Rα and IL-13Rα1 are commonly expressed in osteoclast precursors and osteoblasts, while γc is expressed in osteoclast precursors but not in osteoblasts. Palmqvist *et al.* showed that the expression of IL-13Rα2, a decoy receptor for IL-13 signalling, is decreased by treatment with RANKL and M-CSF in BMMs, and recovered by IL-13.[14] Therefore, the expression patterns of the receptor subunits may be related, at least in part, to the inhibitory actions of IL-4 and IL-13 toward osteoclast differentiation.

Moreno *et al.* showed that IC_{50} for IL-4 induced suppression of osteoclast differentiation correlated directly to the EC_{50} for inducing the tyrosine phosphorylation of STAT6.[13] We further revealed that IL-4 induces tyrosine phosphorylation of STAT6 at lower concentrations than IL-13 in osteoclast precursors, while that in osteoblasts was equivalent. These results are consistent with those observed in the analysis of osteoclast differentiation, OPG production and NFATc1 expression. Thus, levels of STAT6 activation may be crucially involved in the inhibition of osteoclast differentiation. Further investigation including the analysis of JAK3 phosphorylation is required to reveal the precise roles of intracellular signalling pathways in the regulation of osteoclast differentiation.

Osteoclast precursors are multipotential cells that differentiate into immune cells, such as mature macrophages and dendritic cells.[9,28] Although NFATc1 has been reported to regulate osteoclast differentiation induced by RANKL, the factor is also involved in immune cell functions.[29] Our RT–PCR analysis showed that a concentration of 10 ng/ml of IL-4, but not IL-13, inhibited NFATc1 expression in osteoclast precursors. Therefore, we concluded that IL-4 and IL-13 differently regulate the balance of differentiation into immune cells and osteoclasts via NFATc1.

Recently, Ahn *et al.* reported that IL-4 was more effective than IL-13 for *in vitro* differentiation of dendritic cells from peripheral blood mononuclear cells.[30] We also found that the inhibitory effects of IL-4 and IL-13 are different toward osteoclast precursors, while they are equivalent toward osteoblasts for the induction of OPG production. Together, our results imply that IL-4 and IL-13 play different roles in bone metabolism, including inhibition of bone resorption.

Acknowledgements

We thank Dr Achsah D. Keegan (University of Maryland) for the critical review of our manuscript. We also thank Drs Yongwon Choi (University of Pennsylvania) and Charles A. O'Brien (University of Arkansas for Medical Sciences) for providing the soluble forms of human

TRANCE and UAMS-32 cells, respectively. This work was supported in part by the 'High-Tech Research Center' Project for Private Universities matching fund subsidy, as well as grants-in aid from the Ministry of Education, Culture, Sports, Science and Technology of Japan.

References

1 Suda T, Takahashi N, Udagawa N, Jimi E, Gillespie MT, Martin TJ. Modulation of osteoclast differentiation and function by the new members of the tumor necrosis factor receptor and ligand families. *Endocr Rev* 1999; **20**:345–57.

2 Simonet WS, Lacey DL, Dunstan CR *et al.* Osteoprotegerin: a novel secreted protein involved in the regulation of bone density. *Cell* 1997; **89**:309–19.

3 Tsuda E, Goto M, Mochizuki S, Yano K, Kobayashi F, Morinaga T, Higashio K. Isolation of a novel cytokine from human fibroblasts that specifically inhibits osteoclastogenesis. *Biochem Biophys Res Commun* 1997; **234**:137–42.

4 Yasuda H, Shima N, Nakagawa N *et al.* Identity of osteoclastogenesis inhibitory factor (OCIF) and osteoprotegerin (OPG): a mechanism by which OPG/OCIF inhibits osteoclastogenesis *in vitro*. *Endocrinology* 1998; **139**:1329–37.

5 Bucay N, Sarosi I, Dunstan CR *et al.* osteoprotegerin-deficient mice develop early onset osteoporosis and arterial calcification. *Genes Dev* 1998; **12**:1260–8.

6 Mizuno A, Amizuka N, Irie K *et al.* Severe osteoporosis in mice lacking osteoclastogenesis inhibitory factor/osteoprotegerin. *Biochem Biophys Res Commun* 1998; **247**:610–5.

7 Takahashi N, Akatsu T, Udagawa N, Sasaki T, Yamaguchi A, Moseley JM, Martin TJ, Suda T. Osteoblastic cells are involved in osteoclast formation. *Endocrinology* 1988; **123**:2600–2.

8 Yasuda H, Shima N, Nakagawa N *et al.* Osteoclast differentiation factor is a ligand for osteoprotegerin/osteoclastogenesis-inhibitory factor and is identical to TRANCE/RANKL. *Proc Natl Acad Sci USA* 1998; **95**:3597–602.

9 Takami M, Kim N, Rho J, Choi Y. Stimulation by toll-like receptors inhibits osteoclast differentiation. *J Immunol* 2002; **169**:1516–23.

10 Mundy GR. Role of cytokines in bone resorption. *J Cell Biochem* 1993; **53**:296–300.

11 Wills-Karp M. Immunologic basis of antigen-induced airway hyperresponsiveness. *Annu Rev Immunol* 1999; **17**:255–81.

12 Callard RE, Matthews DJ, Hibbert L. IL-4 and IL-13 receptors: are they one and the same? *Immunol Today* 1996; **17**:108–10.

13 Moreno JL, Kaczmarek M, Keegan AD, Tondravi M. IL-4 suppresses osteoclast development and mature osteoclast function by a STAT6-dependent mechanism: irreversible inhibition of the differentiation program activated by RANKL. *Blood* 2003; **102**:1078–86.

14 Palmqvist P, Lundberg P, Persson E, Johansson A, Lundgren I, Lie A, Conaway HH, Lerner UH. Inhibition of hormone and cytokine-stimulated osteoclastogenesis and bone resorption by interleukin-4 and interleukin-13 is associated with increased osteoprotegerin and decreased RANKL and RANK in a STAT6-dependent pathway. *J Biol Chem* 2006; **281**:2414–29.

15 Wong BR, Besser D, Kim N, Arron JR, Vologodskaia M, Hanafusa H, Choi Y. TRANCE, a TNF family member, activates Akt/PKB through a signaling complex involving TRAF6 and c-Src. *Mol Cell* 1999; **4**:1041–9.

16 Wong BR, Rho J, Arron J *et al.* TRANCE is a novel ligand of the tumor necrosis factor receptor family that activates c-Jun N-terminal kinase in T cells. *J Biol Chem* 1997; **272**:25190–4.

17 Suda T, Jimi E, Nakamura I, Takahashi N. Role of 1α,25-dihydroxyvitamin D_3 in osteoclast differentiation and function. *Methods Enzymol* 1997; **282**:223–35.

18 Yamada A, Sheikh F, Niimi T, DeMayo FJ, Keegan AD, Donnelly RP, Kimura S. Induction of uteroglobin-related protein 2 (Ugrp2) gene expression by the Th2 cytokines IL-4 and IL-13. *J Immunol* 2005; **175**:5708–15.

19 Takayanagi H, Kim S, Koga T *et al.* Induction and activation of the transcription factor NFATc1 (NFAT2) integrate RANKL signaling in terminal differentiation of osteoclasts. *Dev Cell* 2002; **3**:889–901.

20 Watanabe K, Tanaka Y, Morimoto I, Yahata K, Zeki K, Fujihira T, Yamashita U, Eto S. Interleukin-4 as a potent inhibitor of bone resorption. *Biochem Biophys Res Commun* 1990; **172**:1035–41.

21 Nakano Y, Watanabe K, Morimoto I *et al.* Interleukin-4 inhibits spontaneous and parathyroid hormone-related protein-stimulated osteoclast formation in mice. *J Bone Miner Res* 1994; **9**:1533–9.

22 Okada Y, Morimoto I, Ura K, Nakano Y, Tanaka Y, Nishida S, Nakamura T, Eto S. Short-term treatment of recombinant murine interleukin-4 rapidly inhibits bone formation in normal and ovariectomized mice. *Bone* 1998; **22**:361–5.

23 Ahlen J, Andersson S, Mukohyama H, Roth C, Backman A, Conaway HH, Lerner UH. Characterization of the bone-resorptive effect of interleukin-11 in cultured mouse calvarial bones. *Bone* 2002; **31**:242–51.

24 Nagasaki K, Yamaguchi K, Watanabe K, Eto S, Abe K. Interleukin-4 blocks parathyroid hormone-related protein-induced hypercalcemia *in vivo*. *Biochem Biophys Res Commun* 1991; **178**:694–8.

25 Zurawski G, de Vries JE. Interleukin 13, an interleukin 4-like cytokine that acts on monocytes and B cells, but not on T cells. *Immunol Today* 1994; **15**:19–26.

26 Chomarat P, Banchereau J. Interleukin-4 and interleukin-13: their similarities and discrepancies. *Int Rev Immunol* 1998; **17**:1–52.

27 Welhm MJ, Learmonth L, Bone H, Schrader JW. Interleukin-13 signal transduction in lymphohemopoietic cells. *J Biol Chem* 1995; **270**:2012286–96.

28 Miyamoto T, Ohneda O, Arai F, Iwamoto K, Okada S, Takagi K, Anderson DM, Suda T. Bifurcation of osteoclasts and dendritic cells from common progenitors. *Blood* 2001; **98**:2544–54.

29 Wagner EF, Eferl R. Fos/AP-1 proteins in bone and the immune system. *Immunol Rev* 2005; **208**:126–40.

30 Ahn JS, Agrawal B. IL-4 is more effective than IL-13 for in vitro differentiation of dendritic cells from peripheral blood mononuclear cells. *Int Immunol* 2005; **17**:1337–46.

nature
cell biology

DEAD-box RNA helicase subunits of the Drosha complex are required for processing of rRNA and a subset of microRNAs

Toru Fukuda[1,6], Kaoru Yamagata[1,2,6], Sally Fujiyama[1,2,6], Takahiro Matsumoto[1,2], Iori Koshida[1], Kimihiro Yoshimura[1], Masatomo Mihara[1], Masanori Naitou[3], Hideki Endoh[3], Takashi Nakamura[1,2], Chihiro Akimoto[1], Yoko Yamamoto[1], Takenobu Katagiri[4], Charles Foulds[5], Shinichiro Takezawa[1], Hirochika Kitagawa[1], Ken-ichi Takeyama[1], Bert W. O'Malley[5] and Shigeaki Kato[1,2,7]

MicroRNAs (miRNAs) control cell proliferation, differentiation and fate through modulation of gene expression by partially base-pairing with target mRNA sequences[1–6]. Drosha is an RNase III enzyme that is the catalytic subunit of a large complex that cleaves pri-miRNAs with distinct structures into pre-miRNAs[7]. Here, we show that both the p68 and p72 DEAD-box RNA helicase subunits[8–10] in the mouse Drosha complex are indispensable for survival in mice, and both are required for primary miRNA and rRNA processing. Gene disruption of either *p68* or *p72* in mice resulted in early lethality, and in both *p68*$^{-/-}$ and *p72*$^{-/-}$ embryos, expression levels of a set of, but not all, miRNAs and 5.8S rRNA were significantly lowered. In *p72*$^{-/-}$ MEF cells, expression of p72, but not a mutant lacking ATPase activity, restored the impaired expression of miRNAs and 5.8S rRNA. Furthermore, we purified the large complex of mouse Drosha and showed it could generate pre-miRNA and 5.8S rRNA *in vitro*. Thus, we suggest that DEAD-box RNA helicase subunits are required for recognition of a subset of primary miRNAs in mDrosha-mediated processing.

DEAD-box RNA helicases unwind RNA and alter RNA structures through ATP binding and hydrolysis[8–10]. Two members of the family, p68 and p72, have been implicated in many biological events[11–17]. p68 and p72 function may facilitate processing of RNA, particularly miRNA, as generation of miRNAs from primary miRNAs (pri-miRNA) with diverse structures seems to require many RNA-associated factors for RNase III-mediated processing. miRNAs control cell proliferation, differentiation and fate through modulation of gene expression by partially base-pairing with target mRNA sequences[1–6,18]. Mammalian miRNA genes are initially transcribed as mono- or polycistronic precursor pri-miRNAs. Pri-mRNAs are processed into 60–70 nucleotide hairpins with 3'-overhangs by nuclear RNase III endonuclease Drosha to form pre-miRNAs[1,4,7]. Pre-miRNAs translocate into the cytosol and are then processed by Dicer, another RNase III-related enzyme, to form mature 17–24 nucleotide miRNAs[1–7]. Recently, the functional unit of human Drosha (hDrosha) was biochemically identified[7], and it was revealed that hDrosha forms two types of complexes. The smaller di-subunit complex (Drosha plus DGCR8), Microprocessor, mediates genesis of 5.8S rRNA and pre-miRNA from pri-miRNA[7]. The other larger hDrosha complex comprises multiple classes of RNA associated proteins including DEAH-box RNA helicases, heterogeneous nuclear ribonucleoproteins (hnRNP) and several proteins with RNA binding or RRM motifs. p68–p72 ATP-dependent DEAD-box RNA helicases are also components of the larger hDrosha complex[7]. The precise role of the large complex components, particularly the RNA-associated proteins, in processing of pri-miRNA and rRNA remains to be investigated.

The genes for the *p68* and *p72* DEAD-box RNA helicases were disrupted in mice using a conventional method (see Supplementary Information, Fig. S1). The human homologues (DDX5 for p68, refs 8, 9; and DDX17 for p72, ref. 10) are the subunits for the large hDrosha complex[7]. Although no clear phenotypic abnormalities were detected in *p68*$^{+/-}$ and *p72*$^{+/-}$ mice (data not shown), embryonic lethality was observed in *p68*$^{-/-}$ embryos at ~E11.5, and neonatal death occured in *p72*$^{-/-}$ pups (Fig. 1a) at postnatal day 2 (P2) with smaller body size (see Supplementary Information, Fig. S1f). Double disruption of *p68* and *p72* seemed to lead to earlier lethality than *p68* inactivation alone in embryos (Fig. 1a). Ubiquitous expression of p68 and p72 was observed in developing embryos (Fig. 1b). Irrespective of early lethality of the

[1]Institute of Molecular and Cellular Biosciences, University of Tokyo, Yayoi 1-1-1, Bunkyo-ku, Tokyo 113-0032, Japan. [2]ERATO, Japan Science and Technology, Honcho 4-1-8, Kawaguchi, Saitama 332-0012, Japan. [3]Applied Genomics, Molecular Medicine Labs., Drug Discovery Research, Astellas Pharma Inc., 21,Miyukigaoka, Tsukuba-shi, Ibaraki 305-8585, Japan. [4]Research Center for Genomic Medicine, Saitama Medical School, Yamane 1397-1, Hidakashi, Saitama, 350-1242, Japan. [5]Department of Molecular and Cellular Biology, Baylor College of Medicine, One Baylor Plaza, Houston, TX 77030, USA.
[6]These authors contributed equally to this work.
[7]Correspondence should be addressed to S.K. (e-mail: uskato@mail.ecc.u-tokyo.ac.jp)

Received 26 February 2007; accepted 27 March 2007; published online 15 April 2007; DOI: 10.1038/ncb1577

a

Stage	p72	+/+	+/-	-/-
P0		16 (22%)	38 (53%)	18 (25%)
P1		16 (29%)	37 (66%)	3 (5%)
P3		16 (30%)	37 (70%)	0 (0%)
3W		16 (30%)	37 (70%)	0 (0%)

Stage	p68	+/+	+/-	-/-
E10.5		6 (12%)	31 (61%)	14 (27%)
E11.5		6 (30%)	11 (55%)	3 (15%)
E15.5		3 (50%)	3 (50%)	0 (0%)
E17.5		1 (17%)	5 (83%)	0 (0%)

p72	+/+	+/+	+/+	+/-	+/-	+/-	-/-	-/-	-/-
Stage p68	+/+	+/-	-/-	+/+	+/-	-/-	+/+	+/-	-/-
E8.5	4 (18%)	2 (9%)	1 (5%)	1 (5%)	7 (32%)	1 (5%)	3 (13%)	3 (13%)	0 (0%)

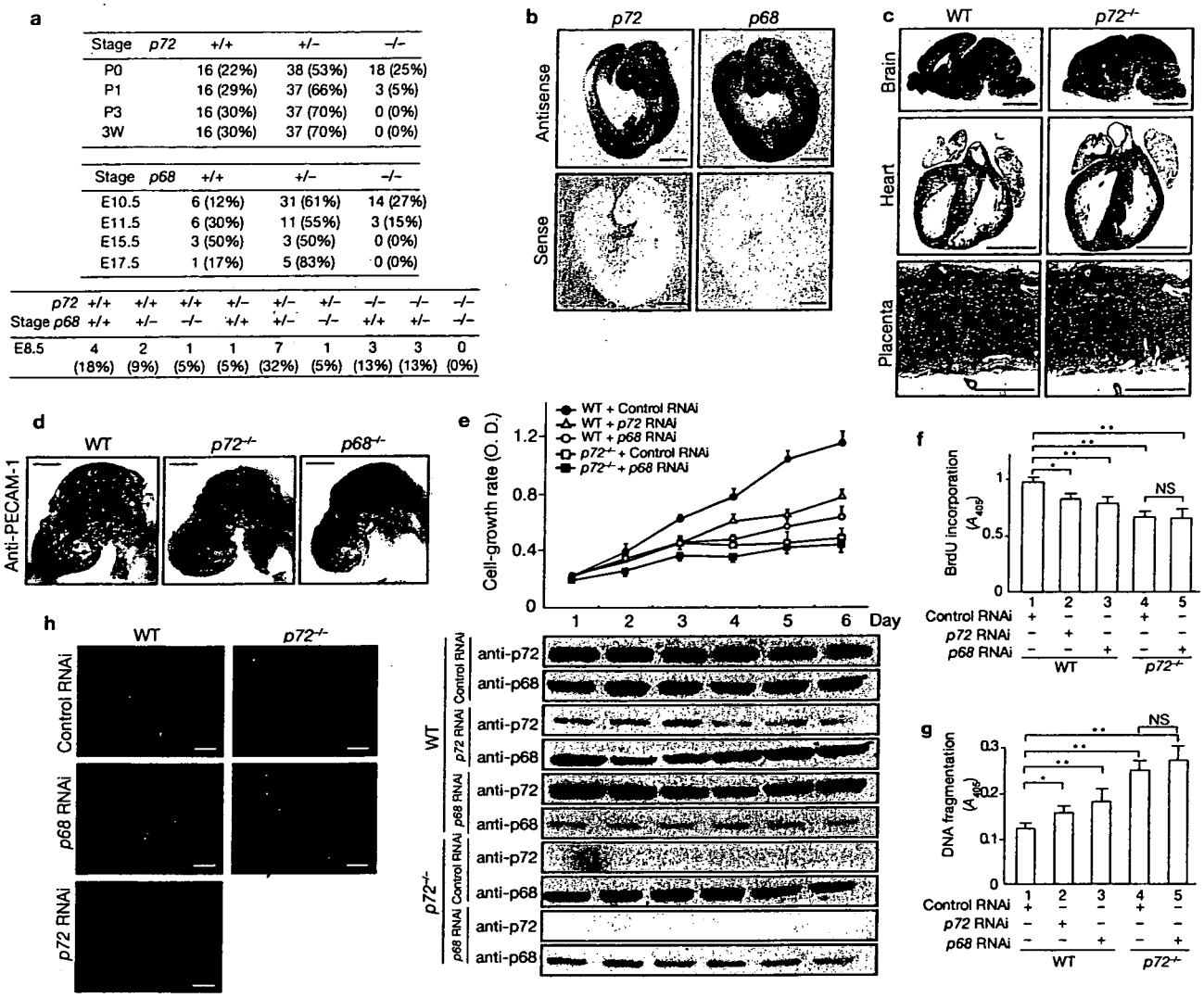

Figure 1 Embryonic and neonatal lethality of *p68* and *p72* knockout mice. (**a**) Genotype of F2 offspring from heterozygous and double (*p68* and *p72*) heterozygous matings. (**b**) Whole-mount *in situ* hybridization of *p72* and *p68* mRNA in wild-type (WT) embryos (E9.5). (**c**) Histological analysis of wild-type and $p72^{-/-}$ embryos (E18.5). Sections were stained with thionine (brain), and hematoxylin and eosin (heart and placenta). (**d**) Immunostaining with anti-PECAM-1 antibody. Wild-type, $p72^{-/-}$ and $p68^{-/-}$ mouse embryos were stage-matched to controls by somite count. (**e**) Analysis of cell-growth rate by modified MTT assay. Results are expressed as the mean ± s.d. of six independent experiments. Protein levels of p72 and p68 for 6 days were confirmed by western blotting. Uncropped images of the blots are shown in the Supplementary Information, Fig. S5a. (**f**) BrdU incorporation of wild-type and $p72^{-/-}$ MEFs with depletion of *p72* and *p68*. Results are expressed as the mean ± s.d. of six independent experiments. Significant differences when compared with the data for wild-type or $p72^{-/-}$ MEFs with control RNAi are shown (single asterisk indicate $P<0.05$; double asterisks indicate $P<0.01$ with one-way ANOVA). NS, not significant. (**g**) Apoptosis was measured by quantification of DNA fragmentation. Results are expressed as the mean ± s.d. of six independent experiments. Significant differences when compared with the data for wild-type or $p72^{-/-}$ MEFs with control RNAi are shown (single asterisk indicates $P<0.05$; double asterisks indicate $P<0.01$with one-way ANOVA). (**h**) TUNEL staining of wild-type and $p72^{-/-}$ MEFs with the indicated RNAi. The scale bars represent 250 μm in **b**, 1 mm in **c**, 150 μm in **d** and 200 μm in **h**.

homozygous mutants, no specific degeneration in organogenesis was detectable (Fig. 1c). Staining with a PECAM-1 antibody showed *p68–p72* homozygous-mutant embryos suffered malformation of blood vessels (Fig. 1d), as previously observed in mice with genetically reduced Dicer activity[19]. Assuming the putative role of the hDrosha complex is in processing of rRNA and miRNAs involved in cellular proliferation, differentiation and cell fate, we first examined cell-growth rates in mouse embryonic fibroblasts (MEFs) from $p72^{-/-}$ embryos. A severe reduction in cell-growth rate because of p72 deficiency was observed (Fig. 1e), and was confirmed by significantly impaired DNA synthesis in $p72^{-/-}$ MEFs, as measured by BrdU incorporation (Fig. 1f). In addition, a clear increase in cell death, as measured by TUNEL staining, was observed in $p72^{-/-}$ MEFs, which was further promoted by *p68* RNA interference (RNAi; Fig. 1g, h).

It has been suggested that the large hDrosha complex containing p68–p72 may, at least in part, excise pri-miRNAs into pre-miRNAs, and cleave preribosomal RNA[7,19–21]. As expression of mature miRNAs was shown to be reduced in human cultured cells deficient in Drosha[20], a global survey of miRNA microarray data was performed to assess expression of miRNAs (www.sanger.ac.uk/Software/Rfam/mirna/index.shtml) in $p72^{-/-}$ embryos at E18.5 (ref. 22). A particular set (94) of pri-miRNAs, but not all surveyed (266), were affected by p72 deficiency (more than 1.5

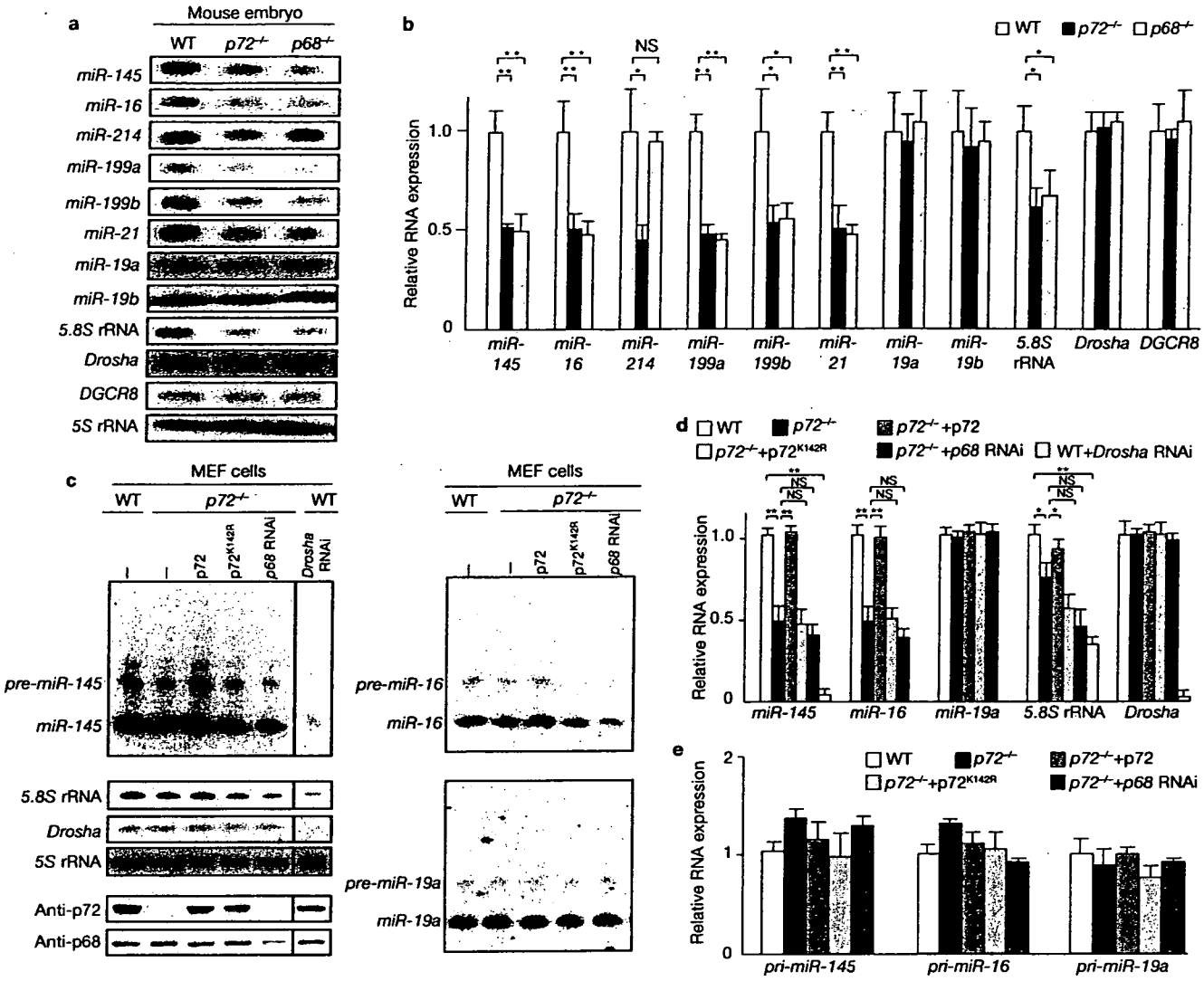

Figure 2 The role of RNA helicases p72 and p68 in miRNA or rRNA processing. **(a)** Northern blot analysis of miRNAs and 5.8S rRNA. Total RNA from wild-type, *p72*$^{-/-}$ and *p68*$^{-/-}$ mouse embryos (E9.5) were purified, and each RNAs were detected by specifc probes as miRNAs, *5.8S* rRNA, *Drosha*, *DGCR8* or *5S* rRNA. **(b)** Results from **a** are expressed as the mean ± s.d. of four independent experiments. Significant differences when compared with the data for wild-type and *p72*$^{-/-}$ or *p68*$^{-/-}$ are shown (single asterisks indicate $P < 0.05$; double asterisks indicate $P < 0.01$ with one-way ANOVA). **(c)** Northern blot analysis of *miRNA-145*, *miRNA-16*, *miRNA-19a*, *5.8S* rRNA, *Drosha* and *5S* rRNA. Total RNA from wild-type or *p72*$^{-/-}$ MEFs transfected with or without the indicated expression vectors were prepared, and each RNA was detected by specific probes as miRNAs, *5.8S* rRNA, *Drosha*, *DGCR8* or *5S* rRNA. The p72 and p68 expression levels in wild-type or *p72*$^{-/-}$ MEFs, with or without the indicated expression vectors, were detected by western blot analysis. Uncropped images of the blots are shown in the Supplementary Information, Fig. S5b. **(d)** Results from **c** are expressed as the mean ± s.d. of four independent experiments. Significant differences when compared with the data for wild-type or *p72*$^{-/-}$ MEFs are shown (single asterisks indicate $P < 0.05$, double asterisk indicates $P < 0.01$ with one-way ANOVA). **(e)** Quantitative RT–PCR analysis of *pri-miR-145*, *15* and *19a* expression in wild-type or *p72*$^{-/-}$ MEFs with indicated expression vectors. Results are expressed as the mean ± s.d. of six independent experiments.

times lowered; see Supplementary Information, Fig. S2). To search homologous motif in the regulated 94 miRNAs, a DNA clustering program (DIALIGN2.2.1, available at http://bibiserv.techfak.uni-bielefeld.de/dialign/) was used. Clustering analysis of the two data sets, revealed no continuous consensus sequence among the miRNAs examined. Expression of several of the miRNAs was detectable at significant levels by northern blot analysis. Deficiency of either p68 or p72 was found to reduce expression levels of *miR-145*, *miR-16*, *miR-199a*, *miR-199b* and *miR-21* to almost half of those in the wild-type littermate embryos (Fig. 2a, b). Likewise, expression levels of 5.8S rRNA were reduced in both homozygous embryos (Fig. 2a, b). However, unlike the miRNAs described above, the expression levels of *miR-19a*, *miR-19b* (Fig. 2a, b), and *miR-32*, *miR-128*, *miR-141* and *miR-146* (data not shown) seemed unaffected by p68–p72 deficiency, and *miR-214* expression was reduced only in *p72*$^{-/-}$, but not in *p68*$^{-/-}$ (Fig. 2a, b).

To verify the putative function of p68 and p72 in RNA processing in embryos, expression levels of these RNAs were then measured in MEF cells from *p72*$^{-/-}$ and wild-type littermate embryos. As expected, a significant reduction in the expression levels of the examined miRNAs and 5.8S rRNA because of p72 deficiency was detected (Fig. 2c, d). Knockdown of Drosha by RNAi (see Supplementary Information, Fig. S3c) caused a reduction in the miRNA expression level (Fig. 2c), as expected. However,

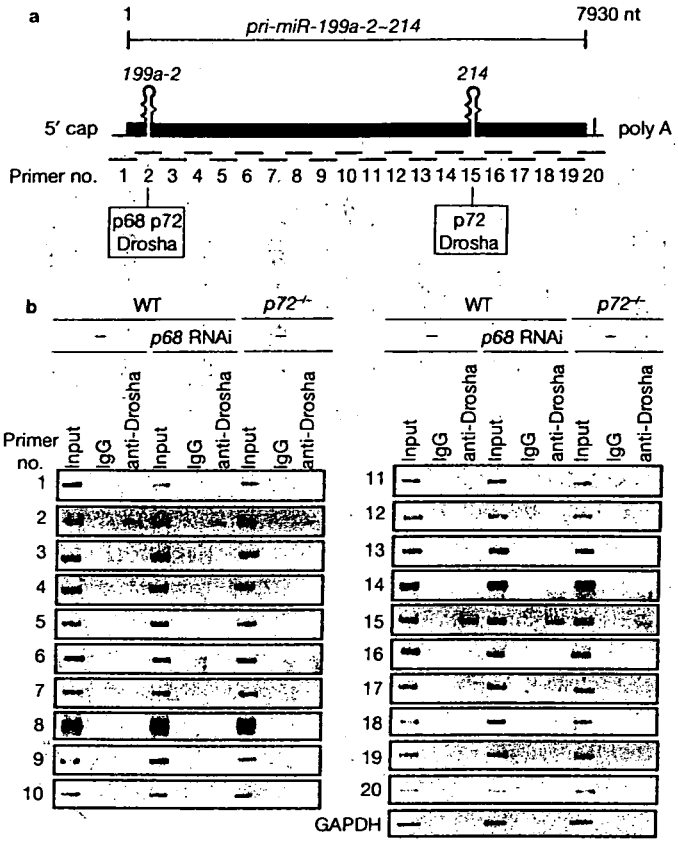

Figure 3 *In vivo* association of the Drosha complex with pri-miRNAs through p68–p72. (a) Schematic representation of *pri-miR-199a-2/-214* with the hairpin structure. The numbers (1–20) under the pri-miRNA indicate the amplified region by PCR with specific primer pairs used for RNA–ChIP analysis in **b**. Binding sites for p68–p72 and Drosha in *pri-miR-199a-2/-214* deduced from the RNA–ChIP analysis in **b** are also indicated. (b) RNA–ChIP analysis of p68–p72 and Drosha binding sites in *pri-miR-199a-2/-214*. ChIP samples were prepared from wild-type MEFs transfected with *p68* RNAi or not, and from $p72^{-/-}$ MEFs. RT–PCR was performed with either total input RNA, RNA precipitated with IgG (negative control) or anti-Drosha antibody.

pri-miRNA-145, *pri-miRNA-16* and *pri-miR-19a* gene expression seemed unaffected by *p72* deficiency plus *p68* RNAi knockdown (Fig. 2e), suggesting that the reduced miRNA levels were not caused by reduced gene expression. Ectopic expression of p72 in $p72^{-/-}$ MEFs was sufficient to restore expression levels of the RNAs, whereas such recovery was not induced by expression of a p72 mutant ($p72^{K142R}$; Fig. 2c, d). $p72^{K142R}$ lacks the putative ATPase activity that is believed essential for RNA helicase activity[10,17]. Knockdown of *p68* and *p72* in the wild-type MEFs clearly lowered expression levels of the miRNAs and 5.8S rRNA, as expected (see Supplementary Information, Fig. S3a), and rRNA processing was significantly affected by *Drosha* RNAi (Fig. 2c). Interestingly, expression levels of *miR-19a* were again unaltered when expression levels of p68–p72 were modulated.

We then addressed the *in vivo* association of pri-miRNAs with p68–p72 in the Drosha complex using an RNA–chromatin immunoprecipiation (ChIP) assay with an mouse Drosha (mDrosha)-specific antibody[23] (Fig. 3b). Using several sets of primers, *in vivo* association of *pri-miR-214* and *pri-mR-16* with Drosha was detected, and the associating regions of pri-miRNAs were mapped (Fig. 3a, b for *pri-miR-214* and see Supplementary Information, Fig. S3b for *pri-miR-16*), although no clearly homologous RNA sequence was present in these regions. Such association was impaired, as expected, in $p72^{-/-}$ MEFs and wild-type MEFs with *p68* knocked down by RNAi (Fig. 3b).

To verify the role of the p68–p72 subunits in the mDrosha complex *in vitro*, the association of endogenous p68–p72 with endogenous mDrosha was confirmed by coimmunoprecipitation (Fig. 4a). DGCR8 coimmunoprecipitated with mDrosha as expected. Using a biochemical approach[24,25], the Drosha complex (Fig. 4b) was purified from nuclear extracts of MCT mouse kidney proximal tubule cells stably expressing Flag- and His-tandem tagged mDrosha at a similar expression level to that of endogenous mDrosha (see Supplementary Information, Fig. S2d). The purified mDrosha complex was present in a single complex with a relative molecular mass of over 670,000 when fractionated on a glycerol density gradient (Fig. 4b). Fractionation of total nuclear extracts with western blotting also showed comigration of endogenous Drosha with DGCR8 and p68–p72 at the similar molecular masses with the purified mDrosha complex (Fig. 4c). These findings are consistent with a previous report that the Drosha complex was biochemically isolated as one large complex from S2 insect cells[26]. However, the small complex corresponding to the human Microprocessor complex was undetectable. Even under more stringent conditions (such as at higher salt concentrations), the smaller mDrosha complex was biochemically undetectable in our hands (data not shown). Using mass spectrometric sequencing, p68–p72, several RNPs and mouse DGCR8 were identified (Fig. 4d), and all of the examined subunits were detected by western blotting analysis (Fig. 4b). Two-step column purification of mDrosha complex identified the same subunits (Fig. 4e), supporting previous reports that p68–p72 form a complex[7,27]. As the subunit composition of the purified mDrosha complex accurately reflects the reported composition of the large hDrosha complex components, we presumed that mDrosha forms one large complex similar to the large hDrosha complex.

We then examined whether this purified large complex mediates the processing of miRNA *in vitro*. The purified complex from fraction 7 (Fr. 7) on the glycerol density gradient (see Fig. 4b), as well as the immunoprecipitates of Drosha (Flag–His–mDrosha; Fig. 5a), were able to cleave *miR-16* and *miR-145* pri-miRNAs into pre-miRNAs (Fig. 5b), but not mRNAs (see Supplementary Information, Fig. S4a). Cleavage products of pre-miRNAs were of the expected size (70 nucleotides for *miR-145*, 93 nucleotides for *miR-16*) and 5.8S rRNA (157 nucleotides) was generated from 12S rRNA *in vitro* (Fig. 5b)[21]. However, conversion efficiency of this *in vitro* RNA processing was unexpectedly low, even for longer incubations (Fig. 5c), raising the possibility that a coregulatory subunit for the mDrosha complex may be lost during biochemical purification. Such *in vitro* RNA processing activity of the purified complex (Fr. 7) was significantly attenuated by specific antibodies for p68–p72, as well as mDrosha (Fig. 5d), and by the presence of an ATP analogue (see Supplementary Information, Fig. S4b, c), supporting ATP dependency (Fig. 5e). Furthermore, the complex deficient of either p68 or p72, purified from stable transformants knocked down with RNAi, was impaired in RNA processing (Fig. 5f). This confirms the significance of p68–p72 subunits within the mDrosha complex in RNA processing.

In this study, early lethality of $p68^{-/-}$ and $p72^{-/-}$ mice clearly establishes the physiological significance of DEAD-box RNA helicases in survival. The physiological impact of p68–p72 on cell differentiation, proliferation and cell fate was also observed in MEFs. Most importantly, the processing of a set of miRNAs and rRNA seemed to

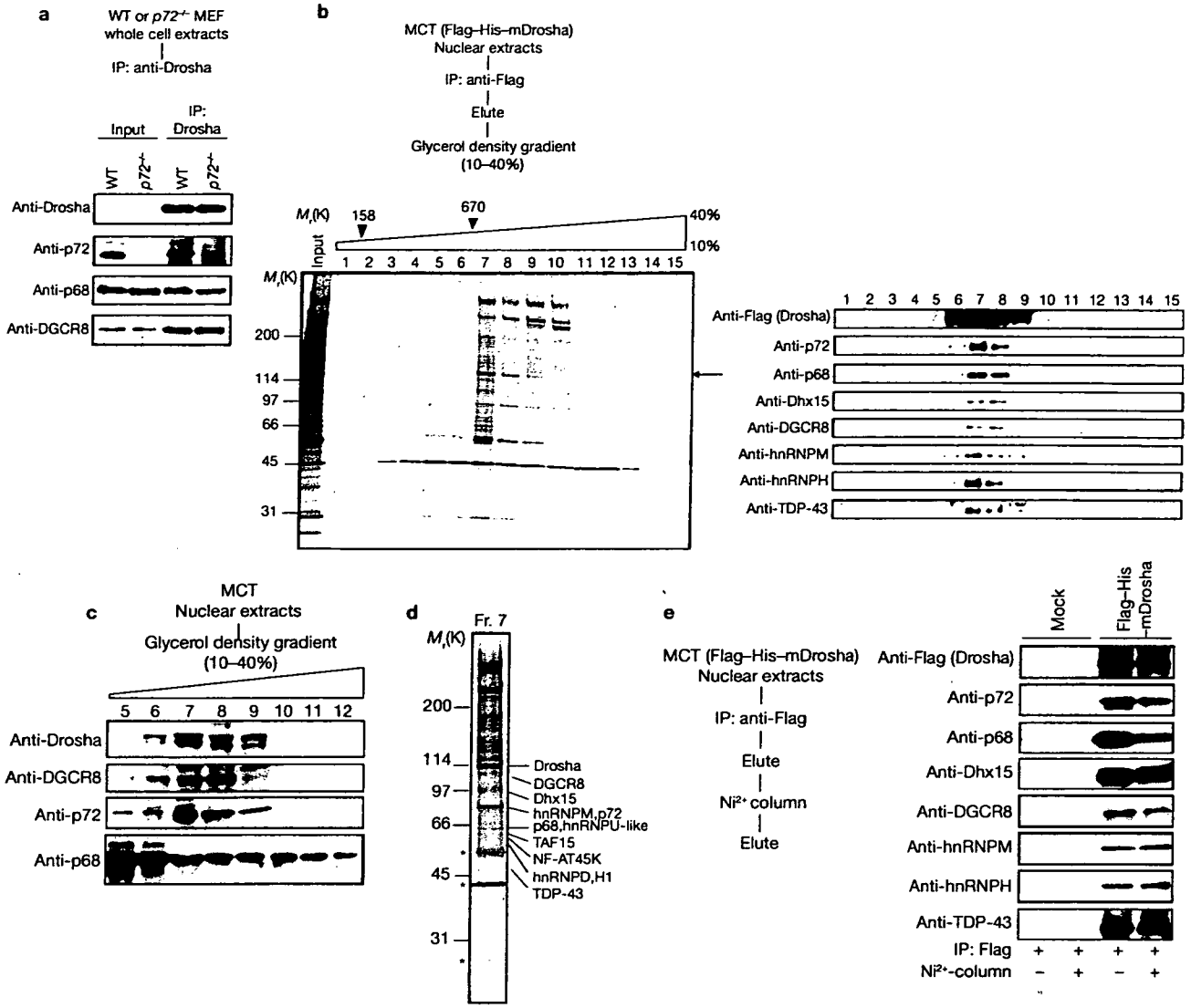

Figure 4 Biochemical isolation of mouse Drosha-containing complex. **(a)** Coimmunoprecipitation of p68–p72 with mDrosha. Whole-cell extracts from MEFs (wild-type and *p72*$^{-/-}$) were prepared for immunoprecipitation (IP) with endogenous mDrosha followed by western blotting (IB). Input, 5% of the cell extracts for immunprecipitation. Uncropped images of the blots are shown in the Supplementary Information, Fig. S5c. **(b)** Biochemical isolation of mouse Drosha-containing complexes. Silver staining and western blot analysis of glycerol density-gradient fractions are displayed. Molecular masses of marker proteins and fraction numbers are indicated. Fraction 7 was used for mass spectrometric analysis and *in vitro* RNA processing. Input, 5% of the input for glycerol density gradient. The arrow indicates Flag–His–mDrosha. **(c)** Endogenous mDrosha, DGCR8, p72 and p68 cosediment at the same fractions with the Flag–His–mDrosha complex on glycerol density gradients. **(d)** Mass spectrometric identifications of the components in Fr. 7 Flag–His–mDrosha complex in **b**. Asterisks indicate background bands. **(e)** Identification of mDrosha complex components in the mDrosha immunoprecipitant. The Flag–His–mDrosha complex was collected from the nuclear extracts using an anti-Flag antibody column, then repurified by Ni^{2+} affinity chromatography. The complex components were analysed by western blot.

be impaired in both of the homozygous mutants (Fig. 2a, b and see Supplementary Information, Fig. S2). Currently, it remains unclear whether the cellular function of affected miRNAs as a result of *p68–p72* knockout is related to early lethality observed in *p68*$^{-/-}$ and *p72*$^{-/-}$ mice. However, considering the previous report that mouse embryogenesis in the absence of Dicer ceases at an earlier stage (E7.5)[28], normal expression of miRNAs may be essential for survival. Furthermore, the purified mDrosha complex containing p68–p72 was capable of generating a set of processed pre-miRNAs and rRNA through p68 and p72 using an *in vitro* assay (Fig. 5b). Impaired miRNA processing was detected for several, but not all, of the examined miRNA species. Therefore, we speculate that p68–p72 DEAD-box RNA helicases serve as miRNA species-selective subunits in the conversion of pri-miRNA into pre-miRNA by specific recognition of a certain structure of pri-miRNA. This hypothesis is supported by a previous report that the double-stranded RNA-binding protein partner of Drosha (Pasha) is required for insect Drosha-mediated pri-miRNA processing[26]. In this respect, it would be interesting to know whether the cellular functions of the specific miRNAs species processed by p68–p72 correlate with the putative biological functions of p68–p72 (refs 11–17).

Different sets of RNA-associated protein subunits may be required for the processing of other miRNA species[29]. Notably, in the p68–p72 homozygous mutants, the expression levels of several miRNAs were reduced to only half of the wild-type littermates. Therefore, we

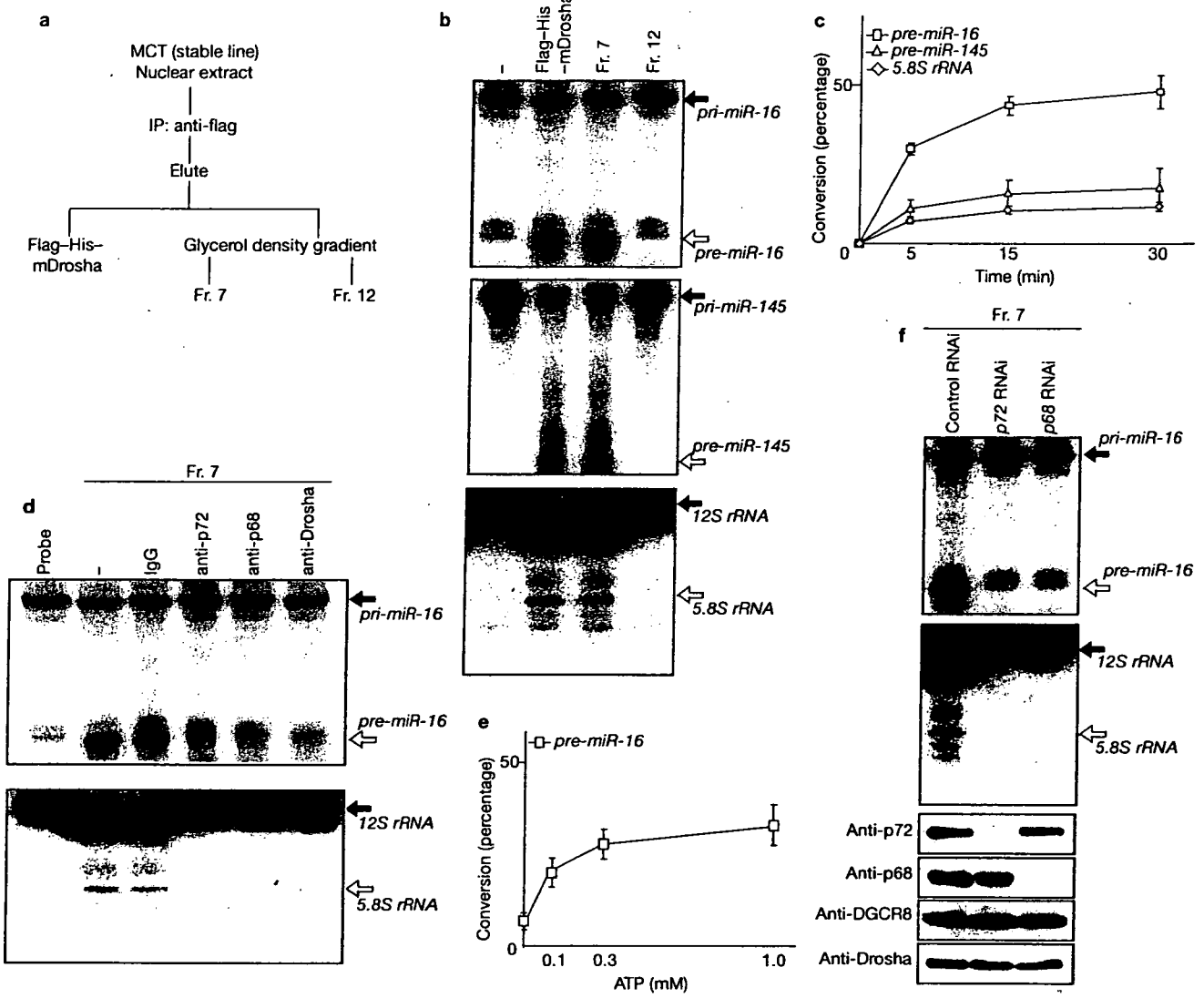

Figure 5 Purified mDrosha complex mediates processing of miRNA and rRNA *in vitro*. **(a)** Schematic representation of the preparation of the samples used in **b**. **(b)** *In vitro* processing analysis of *pri-miR-16*, *pri-miR-145* and *12S* rRNA with Flag–HIS–mDrosha immunocomplexes, fractionated mDrosha complex (Fr. 7), mDrosha-negative fraction (Fr. 12) or negative control (–). Closed arrows and opened arrows indicate the precursor RNA and processed RNA, respectively. **(c)** Time-course conversion rate of *pre-miR-16*, *pre-miR-145* and *5.8S* rRNA (diamond) by purified mDrosha complex (Fr. 7). Results are expressed as the mean ± s.d. of three independent experiments. **(d)** Specific antibodies for p68, p72 and mDrosha attenuated the *pri-miR-16* and *12S* rRNA cleavage by the purified mDrosha complex (Fr. 7). All studies were repeated three times. Probe, input of the substrate *pri-miR-16*; –, Fr. 7 only; IgG, negative control. Closed arrows and opened arrows indicate the precursor RNA and processed RNA, respectively. **(e)** ATP concentration-dependent effect on the *pri-miR-16* cleavage by purified mDrosha complex (Fr. 7). Results are expressed as the mean ± s.d. of three independent experiments. **(f)** *In vitro* processing analysis of *pri-miR-16* and *12S* rRNA with the purified mDrosha complexes prepared from Flag–His–mDrosha stable cells transfected with control RNAi, *p72* RNAi or *p68* RNAi. Western blotting indicates the presence of each complex component. Closed arrows and opened arrows indicate the precursor RNA and processed RNA, respectively. Uncropped images of the blots are shown in the Supplementary Information, Fig. S5d.

speculate that there is possible functional redundancy of p68–p72 with other RNA processing subunits. As it is known that nuclear complexes often form subclasses through association of core components with regulatory subunits[30,31], we cannot exclude the possibility that Drosha–DGCR8 exist as multiple complexes differentially combined with RNA-associated protein subunits in mammals. Furthermore, the subunit composition of the Drosha complex may be developmentally modulated, and thereby cell-type specific.

It remains unclear how the p68–p72 subunits support RNA processing activity of the complex. p68–p72 may function to specifically recognize and stably bind to certain structures of pri-miRNAs and 12S pre-rRNA, and to initiate cleavage at precise RNA sites by Drosha. As the p72 mutant lacking putative ATPase activity did not potentiate RNA processing (Fig. 2c, d), we suggest that ATPase activity of p68–p72 may be required. p68–p72 ATPase activity is dependent on RNA binding[10,32] and is likely to be critical for RNA-unwinding activity[3]. Therefore, we suggest that ATP-dependent p68–p72-mediated structural alteration of specifically associating protein subunits may lead to presentation of RNAs for cleavage by mammalian Drosha. DGCR8 has been reported to be a critical pri-miRNA-associated subunit for Drosha to precisely recognize miRNA stem-loop structures[7,33]. However, other RNA-associated subunits may recognize distinct cognate pri-miRNA tertiary structures by similar or different mechanisms, thus enabling the Drosha complex to process a number of pri-miRNAs. □

METHODS

Antibodies. The following antibodies were used: p68-ab10261 (Abcam, Cambridge, UK); p72 p72N (ref. 17); PECAM-1 MEC13.3 (BD Bioscience, San Jose, CA); Drosha 07017 (Upstate, Billerica, MA); Flag polyclonal (Sigma, St Louis, MO); TARDBP 2E2-D3 (Abnova, Taipei City, Taiwan); hnRNP H N16 (Santa Cruz Biotechnology, Santa Cruz, CA); DHX15 BL972 (Bethyl Laboratories, Montgomery, TX); hnRNP M1-M4 (Zymed, San Francisco, CA); Actin I19 (Santa Cruz). Anti-DGCR8 antibody was generated against a synthetic peptide corresponding to the carboxy-terminal 20 amino-acid sequence (Operon, Huntsville, AL). Appropriate anti-mouse, anti-rabbit and anti-goat secondary antibodies were obtained from Dako (Glostrup, Denmark).

Isolation of MEFs, MEF growth, BrdU incorporation, TUNEL assay and DNA fragmentation. MEFs were isolated from E13.5 embryos and cultured in DMEM with 10% FBS[34]. For MEF growth experiments, cells were seeded in 96-well plates and growth rates were measured by using Cell Counting Kit-8 (Dojindo Laboratories, Kumamoto, Japan). DNA synthesis was detected and measured in cultured cells by BrdU incorporation using 5′-bromo-2′-deoxy-uridine Labeling and Detection Kit III (Roche Applied Science, Basel, Switzerland). Apoptotic cells were assessed by the DNA terminal nick-end translation method (TUNEL assay) using the DeadEnd Fluorometric TUNEL System (Promega, Madison, WI). For apoptotic cell quantitation, DNA fragmentation was measured by using Cell Death Detection ELISA^{PLUS} (Roche Applied Science). These assays were performed following the manufacturer's instructions.

RNAi depletion of *p68*, *p72* and *Drosha*. Small interfering RNA (siRNA) oligonucleotides of *p68*, *p72* and *Drosha* were used for knockdown of endogenous protein expression using siGENOME (Dharmacon, Lafayette, CO). Four kinds of independent siRNA duplexes were mixed. Their sequences are: *p68* siRNA duplex, sense 5′-GAACUGAGUGCAAACCAUAUU-3′ and antisense 5′-PUAUGGUUUGCACUCAGUUCUU-3′: sense 5′-GCUUGUCGCUUGAAGUCUAUU-3′ and antisense 5′-PUAGACUUCAAGCGACAAGCUU-3′: sense 5′-UCAAUUAUGACUACCCUAAUU-3′ and antisense 5′-PUUAGGGUAGUCAUAAUUGAUU-3′;sense5′-GCGCACCGCACAAGAGGUAUU-3′ and antisense 5′-PUACCUCUUGUGCGGUGCGCUU-3′. *p72* siRNA duplex: sense 5′-GUACUUACCUUGUGUUGGAUU-3′ and antisense 5′-PUCCAACACAAGGUAAGUACUU-3′;sense5′-GAAAGAGAUUGGGUACUUAUU-3′ and antisense 5′-PUAAGUACCCAAUCUCUUUCUU-3′; sense 5′-GGAAGACAUUGGCGUAUUUUU-3′ and antisense 5′-PAAAUACGCCAAUGUCUUCCUU-3′;sense5′-GGGCUAGGUUUGUAUAGAUUU-3′ and antisense 5′-PAUCUAUACAAACCUAGCCCUU-3′. *Drosha* siRNA duplex: sense 5′-CGUGGAGGGUGUUAUAGUAUU-3′ and antisense 5′-PUACUAUAACACCCUCCACGUU-3′;sense5′-CAAUACGUGUCAUAGAAUGUU-3′ and antisense 5′-PCAUUCUAUGACACGUAUUGUU-3′: sense 5′-GAACCUACAUCGUGAGCGGUU-3′ and antisense 5′-PCCGCUCACGAUGUAGGUUCUU-3′;sense5′-GGGACUCUCUAGACUGUGAUU-3′and antisense 5′-PUCACAGUCUAGAGAGUCCCUU-3′. MEFs were transfected with each duplex (25 nM) using SuperFect transfection reagent (Qiagen, Hilden, Germany).

Northern blot analysis and quantitative RT–PCR. Total RNA from embryos or MEFs was prepared in TRIzol reagents (Invitrogen, Carlsbad, CA) in accordance with the manufacturer's instructions. Northern blot analysis was carried out as previously described[35]. *Drosha* cDNA and the following oligonucleotides were used as probes: *miR-145*, 5′-AAGGGATTCCTGGGAAAACTGGAC-3′; *miR-16*, 5′-CGCCAATATTTACGTGCTGCTA-3′; *miR-214*, 5′-CTGCCTGTCTGTGCCTGCTGT-3′; *miR-199a*, 5′-AACCAATGTGCAGACTACTGTA-3′; *miR-199b*, 5′-GAACAGGTAGTCTAAACACTGGG-3′; *miR-21*, 5′-TCAACATCAGTCTGATAAGCTA-3′; *miR-19a*, 5′-TCAGTTTTGCATAGATTTGCACA-3′; *miR-19b*, 5′-TCAGTTTTGCATGGATTTGCACA-3′; *5.8S* rRNA, 5′-TCAGACAGGCGTAGCCCCGGGAGGAACCCG-3′; and *5S* rRNA, 5′-CAGGCCCGACCCTGCTTAGCTTCCGAGATCAGACGAGAT-3′(5S rRNA). Real-time quantitative RT–PCR was performed on an ABI Prism 7900HT Sequence Detector (Applied Biosystems, Foster City, CA). The primers used were as follows: *pri-miR-16*, 5′-CCCTTGGAGTAAAGTAGCAGCA-3′ (forward) and 5′-GTCCTTGTATTTTGAGGCAGCA-3′ (reverse); *pri-miR-19*, 5′-ACTGCCCTAAGTGCTCCTTCTG-3′ (forward) and 5′-GAGGGCTGCAAACACAACTATG-3′(reverse); *pri-miR-145*, 5′-ATGCCGAGAGAACTGCTGGT-3′ (forward) and 5′-AAACTGGACCGTGAGGACAA-3′(reverse); *GAPDH*, 5′-AAATGGTGAAGGTCGGTGTG-3′(forward) and 5′-TGAAGGGGTCGTTGATGG-3′ (reverse). Expression levels were normalized for GAPDH expression.

Purification of Flag–His–mDrosha. Flag–His–mDrosha was transfected into MCT mouse kidney proximal tubule cells. Transfected cells were selected with G418 and individual colonies were isolated and analysed for Flag–His–mDrosha expression. To purify the mDrosha complex, nuclear extract was prepared as described previously[24,25] and applied to the anti-Flag M2 affinity resin (Sigma) column. After washes with buffer A (20 mM Tris–HCl at pH 7.9, 0.5 M KCl, 10% glycerol, 1 mM EDTA, 5 mM DTT, 0.5% NP-40, 0.2 mM PMSF), the affinity column was eluted with 400 μg ml^{-1} Flag peptide in buffer A. Eluted complex was analysed by 10–40% glycerol density gradient centrifugation. Fractions from the glycerol density gradient were concentrated by precipitation with trichloroacetic acid and analysed by SDS–PAGE followed by silver staining and western blotting[24,25]. For two-step purification, Flag-eluted complex was applied to HIS–Select nickel affinity gel (Sigma). After washes with 0.8× LEW buffer (40 mM NaH_2PO_4 at pH 8.0, 240 mM NaCl), the complex was eluted with elution buffer (50 mM NaH_2PO_4 at pH 8.0, 300 mM NaCl, 250 mM imidazole). For the large mDrosha complex deficient for p68 or p72, *p68* or *p72* was knocked down by RNAi in the stable transformants before the complex purification.

***In vitro* miRNA or rRNA processing analysis.** *In vitro* transcription was carried out using linearized pcDNA3 vector containing *pri-miR-16* or *12S* rRNA[24]. Briefly, the miRNA probes (*pri-miR-16* or *pri-miR-145*) were amplified from embryo RNA by RT–PCR with 5′-TTCAGGGATCCCATGCTAGCAAGAAGCACTTGGCCA-3′ as forward primer and 5′-AACAAGAATTCTGAAAAGGTGCAGGCCATACTGTGC-3′ as reverse primer or 5′-TTCAGGGATCCAAAAGCTATACAAAGGTCAGAAGAG-3′ as forward primer and 5′-AACAAGAATTCTTCCCAGAGCAGGACGCTGCATCCC-3′as reverse primer, respectively. The *12S* rRNA probes were also prepared with 5′-TCTATGGATCCGTCAGAAAGGGGGGACACGCGCCCAGCCGC-3′as forward primer and 5′-TCTATGAATTCCGACTCTTAGCGGTGGATCACTCGGCTCGTG-3′ as reverse primer. The processing reaction, containing the indicated amounts of Drosha complex (immunoprecipitation products or two-step purification products from MCT cells), 3 μl of solution containing 32 mM $MgCl_2$, 10 mM ATP, 2006mM creatine phosphate, 20 U μl^{-1} RNAase inhibitor (Toyobo, Osaka, Japan) and the α^{32}P-UTP-internal-labelled pri-miRNA and buffer (20 mM Tris–HCl at pH 7.9, 0.1 M KCl, 10% glycerol, 5 mM DTT, 0.2 mM PMSF), were added to a final volume of 30 μl, as previously described[7,20], in the absence or presence of hexokinase (Sigma). The reaction mixture was incubated at 37 °C for 90 min and extracted with phenol:chloroform mixture, then with chloroform and precipitated with 300 mM sodium acetate and ethanol. The precipitated RNA was loaded on 15% denaturing polyacrylamide gels, and then autoradiographed.

RNA–ChIP. RNA–ChIP was performed as previously described[23]. All the buffers used in this study contained 0.5 U μl RNase inhibitor. Nuclei from MEF cells (wild-type, *p68*-knocked down wild-type or *p72*$^{-/-}$) were first isolated from 1% formaldehyde-fixed cells and used for chromatin fragmentation. After immunoprecipiation with anti-Drosha antibody, washing and elution, the precipitated RNA–DNA pellets were resuspended in 70 μl nuclease-free water with 1 μl of 40 U μl^{-1} RNase inhibitor, 5 μl of 1 M Tris–HCl at pH 7.5, 20 μl of 50 mM $MgCl_2$, and 4 μl of 10 U μl DNase I. The mixture was incubated for 30 min at 37 °C and extracted once with phenol:chloroform (5:1). RNA was precipitated with ethanol and dissolved in 30 μl of nuclease-free water. Twenty-nine microliters of the RNA was used for a 60 μl cDNA synthesis reaction. The PCR reactions were performed at 33 cycles, which was within the linear range of the amplification. Of 50 μl of product, 6 μl was loaded onto a 1.5% agarose gel, stained with ethidium bromide, and photographed. The primer sequences used are given in the Supplementary Information.

Microarray data. The microarray data can be be seen in ArrayExpress (accession number, E-MEXP-1052; for further details see Supplementary Information, Methods).

Statistical analysis. Statistical differences were determined using one-way ANOVA followed by post-hoc comparison with the Fisher's protected least significant difference test. Statistical significance is displayed as $P < 0.05$ (one asterisk) or $P < 0.01$ (two asterisks).

Note: Supplementary Information is available on the Nature Cell Biology website.

ACKNOWLEDGEMENTS

We thank T. Watanabe, H. Shiina, J. Miyamoto, K. Sekine, R. Fujiki, Y. Imai and S. Tanaka for generation of knockout mice, and H. Higuchi for manuscript preparation. This work was supported in part by the Program for Promotion of Basic Research Activities for Innovative Biosciences (PROBRAIN) and priority areas from the Ministry of Education, Culture, Sports, Science and Technology (to S.K.).

AUTHOR CONTRIBUTIONS

The experimental concept was developed by S.K., B.W.O.M, S.T., K.T., H.E. and H.K. T.F., K.Y. and S.F. conducted most of experiments, and I.K., K.Y., M.M., M.N., T.N., C.A., Y.Y., T.K., C.F. and S.T. contributed materials and supported several experiments. S.K., T.F., K.Y. and S.F. wrote the manuscript.

COMPETING FINANCIAL INTERESTS

The authors declare that they have no competing financial interests.

Published online at http://www.nature.com/naturecellbiology/
Reprints and permissions information is available online at http://npg.nature.com/reprintsandpermissions/

1. Carthew, R. W. Gene regulation by microRNAs. *Curr. Opin. Genet. Dev.* **16,** 203–208 (2006).
2. Cullen, B. R. Transcription and processing of human microRNA precursors. *Mol. Cell* **16,** 861–865 (2004).
3. Filipowicz, W., Jaskiewicz, L., Kolb, F. A. & Pillai, R. S. Post-transcriptional gene silencing by siRNAs and miRNAs. *Curr. Opin. Struct. Biol.* **15,** 331–341 (2005).
4. Kim, V. N. MicroRNA biogenesis: coordinated cropping and dicing. *Nature Rev. Mol. Cell Biol.* **6,** 376–385 (2005).
5. Valencia-Sanchez, M. A., Liu, J., Hannon, G. J. & Parker, R. Control of translation and mRNA degradation by miRNAs and siRNAs. *Genes Dev.* **20,** 515–524 (2006).
6. Zamore, P. D. & Haley, B. Ribo-gnome: the big world of small RNAs. *Science* **309,** 1519–1524 (2005).
7. Gregory, R. I. *et al.* The Microprocessor complex mediates the genesis of microRNAs. *Nature* **432,** 235–240 (2004).
8. Hirling, H., Scheffner, M., Restle, T. & Stahl, H. RNA helicase activity associated with the human p68 protein. *Nature* **339,** 562–564 (1989).
9. Huang, Y. & Liu, Z. R. The ATPase, RNA unwinding, and RNA binding activities of recombinant p68 RNA helicase. *J. Biol. Chem.* **277,** 12810–12815 (2002).
10. Lamm, G. M., Nicol, S. M., Fuller-Pace, F. V. & Lamond, A. I. p72: a human nuclear DEAD box protein highly related to p68. *Nucleic Acids Res.* **24,** 3739–3747 (1996).
11. Auboeuf, D., Honig, A., Berget, S. M. & O'Malley, B. W. Coordinate regulation of transcription and splicing by steroid receptor coregulators. *Science* **298,** 416–419 (2002).
12. Bates, G. J. *et al.* The DEAD box protein p68: a novel transcriptional coactivator of the p53 tumour suppressor. *EMBO J.* **24,** 543–553 (2005).
13. Causevic, M. *et al.* Overexpression and poly-ubiquitylation of the DEAD-box RNA helicase p68 in colorectal tumours. *Oncogene* **20,** 7734–7743 (2001).
14. Dubey, P. *et al.* The immunodominant antigen of an ultraviolet-induced regressor tumor is generated by a somatic point mutation in the DEAD box helicase p68. *J. Exp. Med.* **185,** 695–705 (1997).
15. Endoh, H. *et al.* Purification and identification of p68 RNA helicase acting as a transcriptional coactivator specific for the activation function 1 of human estrogen receptor alpha. *Mol. Cell Biol.* **19,** 5363–5372 (1999).
16. Kircher, S. G., Kim, S. H., Fountoulakis, M. & Lubec, G. Reduced levels of DEAD-box proteins DBP-RB and p72 in fetal Down syndrome brains. *Neurochem. Res.* **27,** 1141–1146 (2002).
17. Watanabe, M. *et al.* A subfamily of RNA-binding DEAD-box proteins acts as an estrogen receptor alpha coactivator through the N-terminal activation domain (AF-1) with an RNA coactivator, SRA. *EMBO J.* **20,** 1341–1352 (2001).
18. Boehm, M. & Slack, F. A developmental timing microRNA and its target regulate life span in *C. elegans*. *Science* **310,** 1954–1957 (2005).
19. Yang, W. J. *et al.* Dicer is required for embryonic angiogenesis during mouse development. *J. Biol. Chem.* **280,** 9330–9335 (2005).
20. Lee, Y. *et al.* The nuclear RNase III Drosha initiates microRNA processing. *Nature* **425,** 415–419 (2003).
21. Wu, H., Xu, H., Miraglia, L. J. & Crooke, S. T. Human RNase III is a 160-kDa protein involved in preribosomal RNA processing. *J. Biol. Chem.* **275,** 36957–36965 (2000).
22. Han, J. *et al.* The Drosha-DGCR8 complex in primary microRNA processing. *Genes Dev.* **18,** 3016–3027 (2004).
23. Ni, J. Q., Liu, L. P., Hess, D., Rietdorf, J. & Sun, F. L. *Drosophila* ribosomal proteins are associated with linker histone H1 and suppress gene transcription. *Genes Dev.* **20,** 1959–1973 (2006).
24. Kitagawa, H. *et al.* The chromatin-remodeling complex WINAC targets a nuclear receptor to promoters and is impaired in Williams syndrome. *Cell* **113,** 905–917 (2003).
25. Yanagisawa, J. *et al.* Nuclear receptor function requires a TFTC-type histone acetyl transferase complex. *Mol. Cell* **9,** 553–562 (2002).
26. Denli, A. M., Tops, B. B., Plasterk, R. H., Ketting, R. F. & Hannon, G. J. Processing of primary microRNAs by the Microprocessor complex. *Nature* **432,** 231–235 (2004).
27. Ogilvie, V. C. *et al.* The highly related DEAD box RNA helicases p68 and p72 exist as heterodimers in cells. *Nucleic Acids Res.* **31,** 1470–1480 (2003).
28. Bernstein, E. *et al.* Dicer is essential for mouse development. *Nature Genet.* **35,** 215–217 (2003).
29. Lu, J. *et al.* MicroRNA expression profiles classify human cancers. *Nature* **435,** 834–838 (2005).
30. Otte, A. P. & Kwaks, T. H. Gene repression by Polycomb group protein complexes: a distinct complex for every occasion? *Curr. Opin. Genet. Dev.* **13,** 448–454 (2003).
31. Perissi, V. & Rosenfeld, M. G. Controlling nuclear receptors: the circular logic of cofactor cycles. *Nature Rev. Mol. Cell Biol.* **6,** 542–554 (2005).
32. Iggo, R. D. & Lane, D. P. Nuclear protein p68 is an RNA-dependent ATPase. *EMBO J.* **8,** 1827–1831 (1989).
33. Han, J. *et al.* Molecular basis for the recognition of primary microRNAs by the Drosha-DGCR8 complex. *Cell* **125,** 887–901 (2006).
34. Fujiki, R. *et al.* Ligand-induced transrepression by VDR through association of WSTF with acetylated histones. *EMBO J* **24,** 3881–3894 (2005).
35. Ohtake, F. *et al.* Modulation of oestrogen receptor signalling by association with the activated dioxin receptor. *Nature* **423,** 545–550 (2003).

特集　リハビリテーション医療

障害児(者)のリハビリテーション

芳賀信彦*

キーワード　障害児　肢体不自由児　脳性麻痺　二分脊椎

はじめに

2006年度のリハビリテーション（以下，リハ）に関する診療報酬改定において，「障害児（者）リハビリテーション料」という新たな枠組みが設けられた．この枠組みの対象となるのは，表1に示すように多様な疾患あるいは障害である．本稿では，このなかで主に運動器の障害を示す肢体不自由児のリハについて概説する．

Ⅰ．日本における身体障害児の現状とリハに関する問題点

2001年の厚生労働省による調査[1]では，国内の在宅障害児数（18歳未満）は81,900人と推計される．この数は前回（1996年）の調査と比べほぼ横ばいであるが，この間に小児が減少していることを考えると，小児人口に対する割合としては9.1%増加していることになる．これは同年の調査で324万5,000人と推計される在宅身体障害者（18歳以上）数の伸び（7.6%）を上回る伸び率であり，絶対数は少ないとはいえ，障害児に対するリハは現在においても大きな課題である．同じ調査で障害児の障害を種類別にみると，肢体不自由が58.2%，聴覚・言語障害が18.6%，内部障害が17.3%，視覚障害が5.9%と肢体不自由が約6割を占めている．しかし，肢体不自由の治療に大きく関わるリハの状況は，この調査では明らかにされていない．

肢体不自由児のリハは多様な場面，施設で行われている．急性期の治療（新生児期を含む発症直後の管理や機能再建の手術など）やそれに伴うリハは大学病院，一般総合病院，小児専門病院などを中心に行われているが，機能再建手術の一部は肢体不自由児施設や整形外科単科の病院でも行われている．回復期・維持期のリハは肢体不自由児施設や療育センターを中心に行われている．また，前述の「障害児(者)リハビリテーション料」は，一定の基準を満たした肢体不自由児施設，重症心身障害児施設，国立高度専門医療センター，独立行政法人国立病院機構の設置する医療機関においてのみ算定が認められている．

こういった複雑な状況のなかで，個々の障害児（者）にとって必ずしも施設間でスムーズな連携が行われているとは限らない．また，多職種によるリハを必要とする患者は，複数の施設で同時期にリハを受けている場合が多い．すなわち，A施設で理学療法と作業療法を受けながら，B施設で言語聴覚療法を受ける，といった場合である．これに関して2007年4月の診療報酬再改定において，「疾患別リハビリテーション又は疾患別リハビリテーション医学管理を一の保険医療機関で実施している場合には，他の保険医療機関で，同一の疾患等に係る疾患別リハビリテーション料又は疾患別リハビリテーション医学管理料は算定できない」との記載が追加

*はが・のぶひこ：東京大学大学院医学系研究科教授（リハビリテーション医学）．昭和62年東京大学医学部卒業．主研究領域／小児リハビリテーション．

表1　障害児(者)リハビリテーション料の対象患者

①脳性麻痺
②胎生期若しくは乳幼児期に生じた脳又は脊髄の奇形及び障害
　脳形成不全，小頭症，水頭症，奇形症候症，二分脊椎等が含まれる
③顎・口腔の先天異常
④先天性の体幹四肢の奇形又は変形
　先天性切断，先天性多発性関節拘縮症等が含まれる
⑤先天性神経代謝異常症；大脳白質変性症
⑥先天性又は進行性の神経筋疾患
　脊髄小脳変性症，シャルコーマリートゥース病，進行性筋ジストロフィー症等が含まれる
⑦神経障害による麻痺及び後遺症
　低酸素性脳症，頭部外傷，溺水，脳炎・脳症・髄膜炎，脊髄損傷，脳脊髄腫瘍，腕神経叢損傷・坐骨神経損傷等回復に長期間を要する神経疾患等が含まれる
⑧言語障害，聴覚障害又は認知障害を伴う自閉症等の発達障害
　広汎性発達障害，注意欠陥多動性障害，学習障害等が含まれる

された．

しかし，その後の疑義解釈に関する通知のなかで，「当分の間，他の保険医療機関において，言語聴覚療法を実施し，言語聴覚療法に係る疾患別リハビリテーション料又は疾患別リハビリテーション医学管理料を算定しても差し支えない」，「障害児(者)リハビリテーションの対象者については，その特殊性を勘案し，障害児(者)リハビリテーション料と疾患別リハビリテーション料をそれぞれ別の医療機関で算定することは可能である」との記載があり，この点は今後も流動的であると考える．

以下，肢体不自由の代表的な疾患である脳性麻痺，二分脊椎について，リハを含む治療の現状と問題点を述べてみたい．

図1　5歳，痙直型両麻痺
両下肢軟部組織解離術を行った後，ギプス固定のまま早期からリハを開始している．

Ⅱ．脳性麻痺

脳性麻痺の定義は旧厚生省研究班によれば，「受胎から新生児期（生後4週以内）に生じる，脳の非進行性病変に基づく，永続的な，しかし変化しうる運動および姿勢の異常である」となっている．近年みられる脳性麻痺児の多くは，痙直型の両麻痺あるいは四肢麻痺であり，四肢・体幹の筋の痙性による運動と姿勢の異常を呈する．この状態のまま異常運動パターンを獲得すると二次的に筋腱の短縮，関節拘縮，関節不適合などを生じ，運動機能はさらに低下する．

そこで痙直型脳性麻痺に対する治療にはリハが大きく関与する．乳幼児期には異常運動パターンの獲得を防ぐため，異常な運動・姿勢の抑制と正常な運動・姿勢の促通を中心としたリハが行われる．幼児期後半から学童期には現実的な移動手段の確立を目標としたリハが行われ，痙性

の程度や二次的な筋腱の短縮・関節拘縮の状態により，整形外科手術などが組み合わされる．整形外科手術は軟部組織の解離による痙性の軽減と関節拘縮や脱臼の改善が目的に行われ，手術後には集中したリハが必要である（図1）．

痙性抑制を目的とした他の治療法として，末梢神経ブロックやボツリヌス毒素注射（日本では四肢への使用は未承認）が行われ，近年は選択的脊髄後根切断術や髄腔内バクロフェン投与が行われることもある．このようにリハを中心としてさまざまな治療法がスムーズに行われるためには，医療施設間の連携が重要である，しかし，小児専門病院を対象にしたアンケート調査では，このような連携が現状では必ずしもスムーズでないことが明らかになっている[2]．周産期医療の進歩により，未熟児に伴う脳室周囲白質軟化症から痙直型両麻痺を生じる例のほか，重度の四肢麻痺の例も増えてきているなかで，地域におけるリハ連携のシステム作りが大切になってきている．

一方，学童期以降になり障害がある程度固定化し，個々の患者の移動手段も確立すると，運動機能の低下は少ないとされ[3]，リハ介入の頻度は少なくなる．しかし，リハ医などによる定期的な診察は必須であり，装具の管理や，成長に伴う関節拘縮の再発や移動能力の低下があれば，装具治療の再検討，一時的なリハの介入などを行う必要がある．成人後の障害についてはあまり知られていない．しかし，重度の障害では生存期間は延びる傾向にあるとされ[4]，適切な健康管理は重要である．アテトーゼ型の脳性麻痺では頸椎症性脊髄症や神経根症のリスクが高く[5]，定期的な診察で神経症状の変化をとらえる必要がある．

Ⅲ．二分脊椎

二分脊椎とは，先天的に脊椎の後方要素（棘突起，椎弓など）が欠損している状態を指し，

図2　2歳，二分脊椎（開放性脊髄髄膜瘤）
内反足のまま立位を取り，足部外側で接地している．

神経管の形成障害・閉鎖不全により生じる．脊髄や馬尾神経が背側に脱出し瘤を形成する嚢胞性二分脊椎では，皮膚欠損を伴うことが多い（開放性あるいは顕在性二分脊椎）．一方，髄膜や神経組織に脱出を伴わないものを潜在性二分脊椎と呼び，神経症状を伴わない場合と，脊髄脂肪腫のように神経症状を伴う場合がある．二分脊椎は神経系の発生異常ととらえることもでき，水頭症，キアリ奇形，脊髄空洞症などを伴うことがある．二分脊椎は腰仙椎部に好発し，下肢の運動麻痺と知覚障害，膀胱直腸障害を示す．診療には脳神経外科，整形外科，リハ科，泌尿器科，小児科，小児外科などのほか，理学療法士，看護師，臨床心理士などが参加したチームアプローチが望ましい．

下肢の運動麻痺は筋力のアンバランスを通じて変形や拘縮の原因となるが，これに中枢神経病変の影響や胎内での肢位による変形が加わるため，病態は複雑である．乳児期のリハとしては，関節拘縮の治療と予防，運動発達の促進を行う．特に大関節の変形・拘縮は後の安定した立位姿勢の妨げになるため（図2），積極的に治

療を行う必要があるが，一方麻痺に伴う骨萎縮があるため無理な矯正は骨折の危険を伴う．必要に応じ整形外科手術や装具治療を組み合わせる．乳児期から幼児期にかけては移動能力のゴールを設定したうえでそれに向けたリハを積極的に行う．

移動能力には麻痺レベル，水頭症，知的障害，褥瘡，脊柱変形，肥満など多くの因子が関与するが，麻痺レベルが最も大きく関与するとされている[6]．杖を使ってでも実用歩行が可能と判断した児に対しては，適切な装具を処方したうえでリハを行うが，変形矯正などを目的とした入院・手術が多くなる傾向がある[7]．高位の麻痺で実用歩行に至らないと判断した患者に対して，立位・歩行のリハを行うことの効果はまだ定まっていない[8]．

二分脊椎では，学童期以降，特に思春期に移動能力が低下することがある．これは成長に伴い脊髄が緊張し下肢の麻痺が悪化すること（脊髄係留症候群）が原因とされることが多いが，ほかにも体重の増加，脊柱変形の進行などが関与する．すなわち，一定の移動能力を獲得した後も，定期的に診察や検査を行う必要がある．二分脊椎患者の成人後の生活や障害に関しては，近年，報告が多くなってきている[9,10]．

文　献

1) 厚生労働省社会・援護局障害保健福祉部：身体障害児・者実態調査結果（平成13年6月1日調査）.（厚生労働省ホームページ：http://www.mhlw.go.jp/houdou/2002/08/h0808-2.html）
2) 芳賀信彦：小児専門病院における脳性麻痺児療育の現状．日小児整外会誌 2006；15：230–234.
3) McCormick A, Brien M, Plourde J, *et al*：Stability of the Gross Motor Function Classification System in adults with cerebral palsy. *Dev Med Child Neurol* 2007；49（4）：265–269.
4) Strauss D, Shavelle R, Reynolds R, *et al*：Survival in cerebral palsy in the last 20 years：signs of improvement? *Dev Med Child Neurol* 2007；49（2）：86–92.
5) Onari K：Surgical treatment for cervical spondylotic myelopathy associated with athetoid cerebral palsy. *J Orthop Sci* 2000；5（5）：439–448.
6) Asher M, Olson J：Factors affecting the ambulatory status of patients with spina bifida cystica. *J Bone Joint Surg Am* 1983；65（3）：350–356.
7) 芳賀信彦，滝川一晴：二分脊椎小児に対する整形外科的治療―入院・手術の調査．日小児整外会誌（印刷中）.
8) Mazur JM, Kyle S：Efficacy of bracing the lower limbs and ambulation training in children with myelomeningocele. *Dev Med Child Neurol* 2004；46（5）：352–356.
9) McDonnell GV, McCann JP：Issues of medical management in adults with spina bifida. *Childs Nerv Syst* 2000；16（4）：222–227.
10) Hetherington R, Dennis M, Barnes M, *et al*：Functional outcome in young adults with spina bifida and hydrocephalus. *Childs Nerv Syst* 2006；22（2）：117–124.

【骨芽細胞】

BMPシグナルによる骨形成
——生理的および病的骨形成への関与
BMP signaling and skeletogenesis

片桐岳信
Takenobu KATAGIRI
埼玉医科大学ゲノム医学研究センター病態生理部門

◎骨形成と骨吸収による骨の代謝はさまざまな因子によって調節されている．なかでも，bone morphogenetic protein(BMP)は筋組織に移植すると異所性の骨形成を誘導する生理活性物質として発見された因子で，これまでに知られている生理活性物質のなかでもっとも強い骨形成を示す因子のひとつである．従来からBMPの異所性骨誘導活性を骨再建に応用することが期待されてきた．しかし，そればかりでなく，BMPに関する最近の研究からBMPシグナルの生理的あるいは病的骨形成における役割が明らかとなりつつある．本稿ではここ数年の骨代謝領域における発見に焦点をあて，BMPの骨形成における新しい役割を考察する．

Key word：BMP，異所性骨形成，骨粗鬆症，変異，細胞内情報伝達，進行性化骨性筋炎

Bone morphogenetic protein(BMP)は，1965年Uristによって筋組織や皮下に移植すると異所性骨形成を誘導する生理活性物質として報告された[1]．1988年にcDNAがクローニングされて以来，これまでにtransforming growth factor-β(TGF-β)スーパーファミリーに属す15種類以上のBMPがクローニングされている[2,3]．BMP-1だけは一次構造がまったく異なり，メタロプロテアーゼの活性をもつ．BMPはさまざまな因子のなかでもっとも強力な骨形成促進因子のひとつであるばかりでなく，初期胚における対軸形成や腎，心臓，眼球などの器官形成おいても重要な役割を担う．

BMPの骨代謝における役割は，BMPおよび受容体などの遺伝子改変マウスや，BMPの移植による異所性骨誘導実験，培養細胞を用いた分化誘導実験などを通して分子レベルで明らかにされてきた．さらに，ヒトやマウスの遺伝性疾患の解析からBMPシグナルの生理的役割が明らかにされた例も多い．本稿では，とくに最近の骨代謝領域における発見にフォーカスを当て，あらたに明らかとなりつつある生理的および病的骨形成におけるBMPシグナルの役割を考察する．

BMPのシグナル伝達

骨形成促進作用をはじめとするBMPの多様な生理活性はすべて，標的細胞上に存在するⅠ型およびⅡ型のセリン・スレオニンキナーゼ型受容体との結合によって細胞内に伝達される[4](図1)．まず，Ⅱ型受容体のキナーゼがⅠ型受容体のグリシンとセリン残基に富むGSドメインとよばれる領域をリン酸化し，これによって活性化されたⅠ型受容体のキナーゼが，細胞質でさらに下流のSmad1/5/8，MAPキナーゼ，PI3キナーゼなどの情報伝達系をリン酸化によって活性化する．最終的にBMPシグナルは，核内における正または負の転写制御として反映される．たとえば，リン酸化Smad1/5/8の核内への集積と，典型的なBMP初期応答遺伝子であるId1の発現は，細胞をBMPで刺激してから約30〜45分後にピークに達する．

細胞外から核内へのBMPシグナルはさまざまな因子によって修飾される(図1)．BMPリガンド

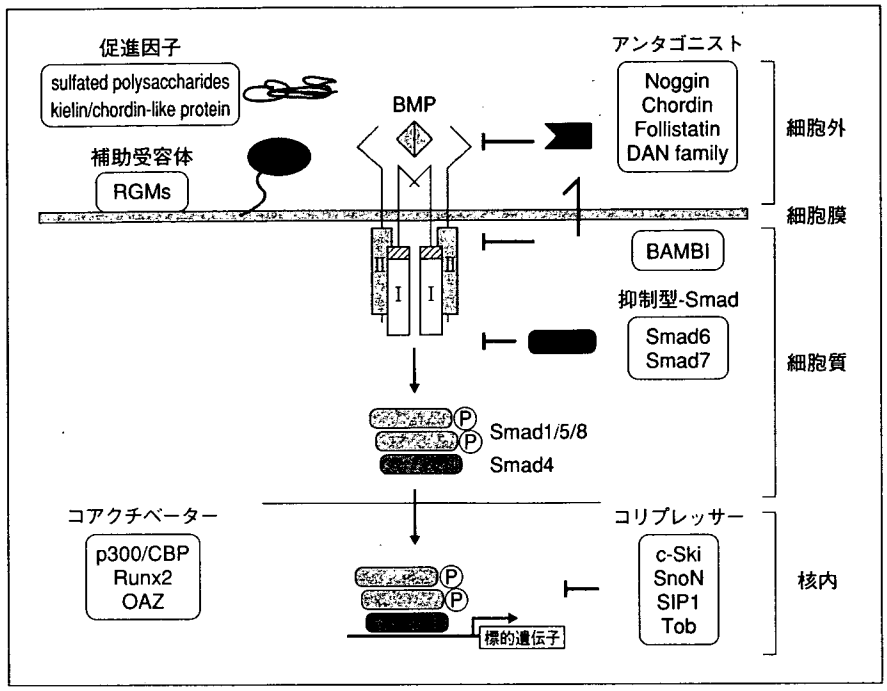

図 1　BMPの細胞内情報伝達系とシグナル修飾因子

BMP は標的細胞のⅠ型とⅡ型受容体に結合する．Ⅱ型受容体はⅠ型受容体の GS ドメイン(斜線の四角)，Ⅰ型受容体は下流の Smad をはじめとする情報伝達系をリン酸化によって活性化する．BMP 活性の修飾因子として，図の左側には活性促進因子，右側には抑制因子を示した．

や受容体自身の発現量の変化ばかりでなく，このような BMP シグナル修飾因子の発現が BMP の生理的役割に深く関与することが明らかとなりつつある．

BMP活性修飾因子

1. 補助受容体

TGF-β の場合，シグナル伝達に関与するⅠ型およびⅡ型受容体のほかに，リガンドと受容体の親和性を高めるⅢ型受容体(補助受容体)の存在が知られている．これまでに，TGF-β の補助受容体として Endoglin や Betaglycan のようなプロテオグリカンが同定されていたが，BMP に対する補助受容体は見出されていなかった．しかし最近，3 種類の repulsive guidance molecule(RGMa，RGMb/DRAGON，RGMc/hemojuvelin/HEF2)がそれぞれ BMP の補助受容体として機能することが明らかとなった[5,6]．

RGM 分子は，C 末端側に GPI アンカーのためのプロペプチドをもつ分泌蛋白質で細胞膜表面上に局在し，BMP リガンドおよびⅠ型受容体と結合することで BMP シグナルを促進する．RGM は生体内で広く発現しているが，RGMb/DRAGON のノックアウトマウスは骨組織に強い表現形質が認められるという．

2. 硫酸化多糖

BMP がヘパリンカラムで精製されることから明らかなように，BMP はヘパリンと高い親和性を示す．一方，ヘパリンはさまざまな生理活性物質と結合し，相手分子の生理活性を相乗的に促進する例が数多く知られている．最近，ヘパリンが *in vitro* および *in vivo* において，BMP の骨芽細胞分化誘導活性や異所性骨誘導活性を促進することが明らかとなった[7-9]．ヘパリンは BMP の分解等を抑制して半減期を延長するとともに，Noggin のような BMP アンタゴニストからリガンドを保護する作用があるらしい[9]．

このヘパリンの作用は分子内の硫酸基に依存しており，同様な分子構造をもつヘパラン硫酸などの硫酸化多糖にもこの活性が認められる．とくにヘパラン硫酸はさまざまな細胞がプロテオグリカンとして細胞膜表面や細胞間基質に発現することから，これらによって BMP 活性が調節されている可能性がある．しかし，培養細胞表面の硫酸化

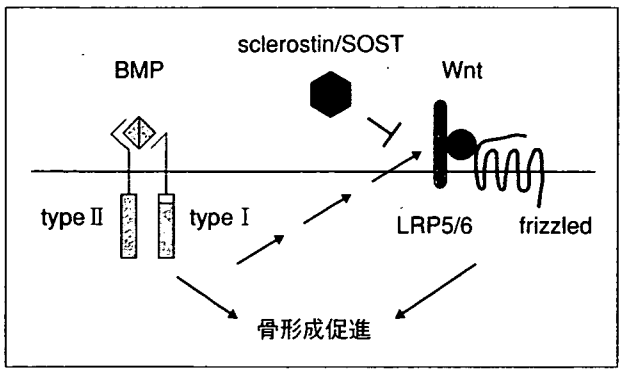

図 2 Sclerostinの活性から予想されるBMPとWntの関係

Sclerostin による BMP 活性御抑制はリガンドに対する直接作用ではなく，下流で活性化される Wnt シグナルの抑制を介する可能性が示唆される．

多糖を分解すると，むしろ BMP 活性が促進されるという報告もある[10]．同じコア蛋白のプロテオグリカンでも各組織によって糖鎖の分子サイズや硫酸化を含めた修飾の多様性が知られており，これらの違いによって BMP 活性が正にも負にも制御される可能性がある．長期間ヘパリンを投与すると骨粗鬆症を惹起することが知られており，BMP 活性との関連が注目される．

3. Sclerostin/SOST

BMP 活性を阻害するアンタゴニストは，Noggin や Chordin をはじめとして数多く同定されている[2](図 1)．これら BMP アンタゴニストのなかで，とくに Sclerostin/SOST に関して最近，新しい展開がみられている．Sclerostin は骨硬化症(sclerosteosis)責任遺伝子の解析から発見された分子で，その後，骨基質のなかの骨細胞が高発現する BMP アンタゴニストであることが報告された[11,12]．最近，骨粗鬆症に対する治療薬のひとつとして Sclerostin の中和抗体が開発されており，卵巣摘出による骨粗鬆症モデルにおいて強力な骨形成促進作用を示すという．

一方，Sclerostin の直接的な標的が BMP ではなく，Wnt であることを示す報告が蓄積しつつある．Wnt 受容体である LRP5 のシグナルは遺伝学的解析からヒトの骨量を調節することが示されていた．最近の報告によると，Sclerostin は Smad のリン酸化など BMP の初期反応を阻害せずに，BMP による異所性骨誘導を阻害するという[13]．Sclerostin が LRP5/6 に結合し，Wnt シグナルを阻害することも示されている[14,15]．これらを総合すると，BMP シグナルの下流で Wnt シグナルが活性化されており，この Wnt シグナルが Sclerostin の標的であると予想される(図 2)．

BMPと骨疾患

1. 骨粗鬆症

遺伝学的解析から，染色体 20p12.3 領域の骨粗鬆症との連鎖が同定されている．ここには BMP-2 がコードされており，塩基配列を解析すると 37 番目のセリン残基からアラニン残基への変異が見出され，これによって BMP-2 蛋白質の安定性や輸送などに変化が起こる可能性が指摘された[16]．しかし最近，さらに大規模な解析から，この BMP-2 の SNP と骨粗鬆症との間には関連がないとの報告がある[17]．また，BMP-2 遺伝子の 3′-UTR 領域内の SNP により結合蛋白との親和性が変化し，mRNA の安定性に差が生じることが示されている[18]．このような転写後の修飾により BMP-2 の発現量が低下し，骨粗鬆症が起こる可能性が考えられる．

BMP は，骨基質に含まれることから，一般に局所的な骨形成因子と考えられている．しかし，血清中にも BMP と類似した生物活性を示す因子が含まれており，この生理活性物質を精製したところ，BMP-4 であることが判明した[19]．この結果は BMP が血流を介して全身性に作用する可能性を示しており，血中 BMP の動態や，BMP の血中レベルと骨代謝との関連が注目される．

2. 骨折

BMP ノックアウトマウスが胎生致死となることから，生後の骨形成における BMP の役割は不明な点が多かった．最近，Tsuji ら[20]は Cre-Lox システムによる四肢特異的な BMP-2 ノックアウトマウスを作製し，とくに生後の骨形成における BMP-2 の重要性を示した．このマウスは胎生期の骨組織の発生はほぼ正常に進行するが，生後に骨折が多発する．さらに，BMP-2 以外の BMP や受容体は正常に発現しているにもかかわらず，軟骨カルスの形成など治癒の初期反応がほとんど認められないことから，BMP-2 は骨折治癒に重要な因子であると結論された[20]．さらに，同様の手法を

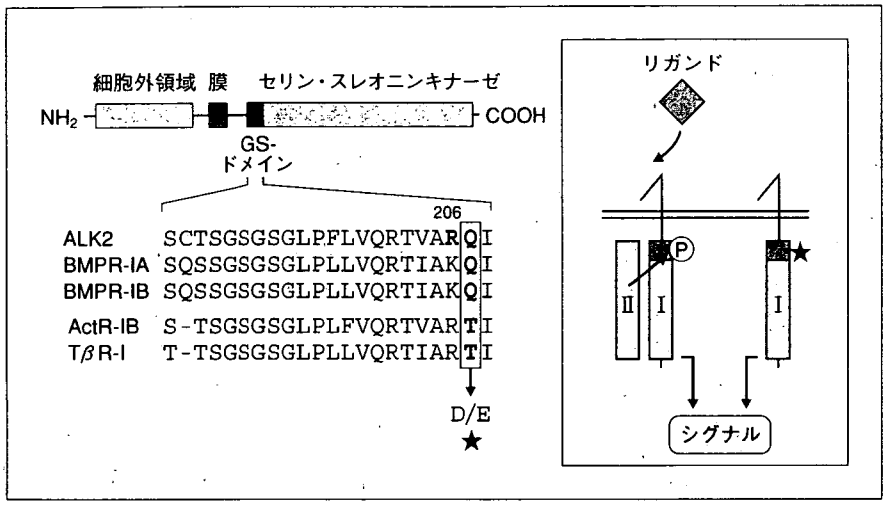

図 3　I 型受容体GSドメインの相同性とアミノ酸置換による活性化
BMP や TGF-β, activin の I 型受容体 GS ドメインは相同性が高い．進行性化骨筋炎で同定された ALK2 の変異 206 は，酸性アミノ酸への置換によって構成的活性化を起こすことが知られていたアミノ酸残基 207 の隣であった．

用いた解析から，BMP-2 と BMP-4 あるいは BMP-2 と BMP-7 をノックアウトしても軟骨形成は正常に起こるが，骨形成には BMP-2 と BMP-4 が必要なことも示されている[21]．

3. 進行性化骨筋炎

進行性化骨筋炎(fibrodysplasia ossificans progressiva：FOP)は，全身の骨格筋が徐々に骨化する常染色体優性遺伝を示す疾患である．この症状が BMP を筋組織に移植した際の異所性骨化と類似していることから，本疾患は BMP シグナルの異常によるものと予想されていた[22]．最近，家族性の進行性化骨筋炎の解析から，I 型 BMP 受容体の一種である ALK2/ACVR1 遺伝子に 617 番目の G から A への変異が同定された[23]．家族性だけでなく，孤発性の症例においても同一の変異が確認されている．この遺伝子上の変異はキナーゼ活性を制御する GS ドメイン内のアミノ酸置換を引き起こし，立体構造の変化を生じる可能性が示された．10 年以上も昔，進行性化骨筋炎で同定された隣のアミノ酸を人為的に酸性アミノ酸に置換すると，TGF-β ファミリーの受容体はリガンド非依存的に活性化されることが報告されている(図 3)[24]．したがって，進行性化骨筋炎では構成的に活性化された BMP 受容体からのシグナルが筋組織の骨化を誘導すると予想される．

おわりに

BMP は発見当初から，整形外科や口腔外科領域などにおける骨再建の促進因子という性格が強かった．しかし本稿で述べたように，ここ数年の間に BMP の生理的あるいは病的骨形成への関与を示すいくつかの発見があった．これにより内科的領域においても BMP が骨形成に重要な調節因子であることが再認識されつつある．骨代謝研究の大きな課題のひとつとして骨カップリングファクターの同定が残されている．この本体が BMP であるかどうかを含めて，今後の研究によって BMP による骨形成調節機構の全体像が明らかとなることが期待される．

文献

1) Urist, M. R.：*Science*, **150**：893-899, 1965.
2) Rosen, V.：*Ann. NY Acad. Sci. USA*, **1068**：19-25, 2006.
3) Abe, E.：*Ann. NY Acad. Sci. USA*, **1068**：41-53, 2006.
4) Wan, M. and Cao, X.：*Biochem. Biophys. Res. Commun.*, **328**：651-657, 2005.
5) Babitt, J. L. et al.：*J. Biol. Chem.*, **280**：29820-29827, 2005.
6) Samad, T. A. et al.：*J. Biol. Chem.*, **280**：14122-14129, 2005.
7) Ruppert, R. et al.：*Eur. J. Biochem.*, **237**：295-302, 1996.
8) Takada, T. et al.：*J. Biol. Chem.*, **278**：43229-43235, 2003.
9) Zhao, B. et al.：*J. Biol. Chem.*, **281**：23246-23253,